viruses

MDPI

Review

The Nucleocapsid of Paramyxoviruses: Structure and Function of an Encapsidated Template

Louis-Marie Bloyet

Department of Molecular Microbiology, School of Medicine, Washington University in Saint Louis, St. Louis, MO 63110, USA; louis-marie.bloyet@wustl.edu

Abstract: Viruses of the *Paramyxoviridae* family share a common and complex molecular machinery for transcribing and replicating their genomes. Their non-segmented, negative-strand RNA genome is encased in a tight homopolymer of viral nucleoproteins (N). This ribonucleoprotein complex, termed a nucleocapsid, is the template of the viral polymerase complex made of the large protein (L) and its co-factor, the phosphoprotein (P). This review summarizes the current knowledge on several aspects of paramyxovirus transcription and replication, including structural and functional data on (1) the architecture of the nucleocapsid (structure of the nucleoprotein, interprotomer contacts, interaction with RNA, and organization of the disordered C-terminal tail of N), (2) the encapsidation of the genomic RNAs (structure of the nucleoprotein in complex with its chaperon P and kinetics of RNA encapsidation in vitro), and (3) the use of the nucleocapsid as a template for the polymerase complex (release of the encased RNA and interaction network allowing the progress of the polymerase complex). Finally, this review presents models of paramyxovirus transcription and replication.

Keywords: paramyxoviruses; nucleocapsid; nucleoprotein; phosphoprotein; polymerase complex; intrinsic disorder

Citation: Bloyet, L.-M. The Nucleocapsid of Paramyxoviruses: Structure and Function of an Encapsidated Template. *Viruses* **2021**, *13*, 2465. https://doi.org/10.3390/v13122465

Academic Editors: Rob W Ruigrok and Martin Blackledge

Received: 17 November 2021
Accepted: 7 December 2021
Published: 9 December 2021

1. Introduction

Members of the *Paramyxoviridae* family are enveloped viruses with non-segmented negative-strand RNA genomes. These viruses share similar gene expression and genome replication mechanisms to the members of the other ten families of the *Mononegavirales* order. Paramyxoviruses are currently divided into 4 subfamilies, 17 genera, and 78 species (Figure 1) [1] (information as of November 2021, for an update see https://talk.ictvonline.org/taxonomy/). Paramyxoviruses are found in a broad range of animals, including mammals, fishes, reptiles, or birds and include several human and animal pathogens such as measles virus (MeV), mumps virus (MuV), canine distemper virus (CDV), and Newcastle disease virus (NDV). Some, such as Nipah virus (NiV) and Hendra virus (HeV), regularly emerge in human or animal populations where they cause deadly epidemics. Although vaccines exist against some paramyxoviruses, effective antiviral treatments for post-exposure prophylaxis are urgently needed [2,3].

Viral transcription and replication are both mediated by an RNA synthesis machinery composed of a viral polymerase complex and its encapsidated template. The polymerase complex consists of the large protein (L) and its co-factor the phosphoprotein (P) [4–7]. This complex uses a genome (or antigenome) embedded into a homopolymer of viral nucleoproteins (N) as a template [8–10]. The encapsidation of the RNA in this ribonucleoprotein structure, known as the nucleocapsid, prevents the annealing of positive and negative RNA strands into double-stranded RNA structures, as well as the folding of genomic RNA into secondary RNA structures, which helps to prevent recognition by innate immune receptors [11,12]. It also protects the genome from degradation by nucleases [13,14] and from being targeted by siRNA [15,16].

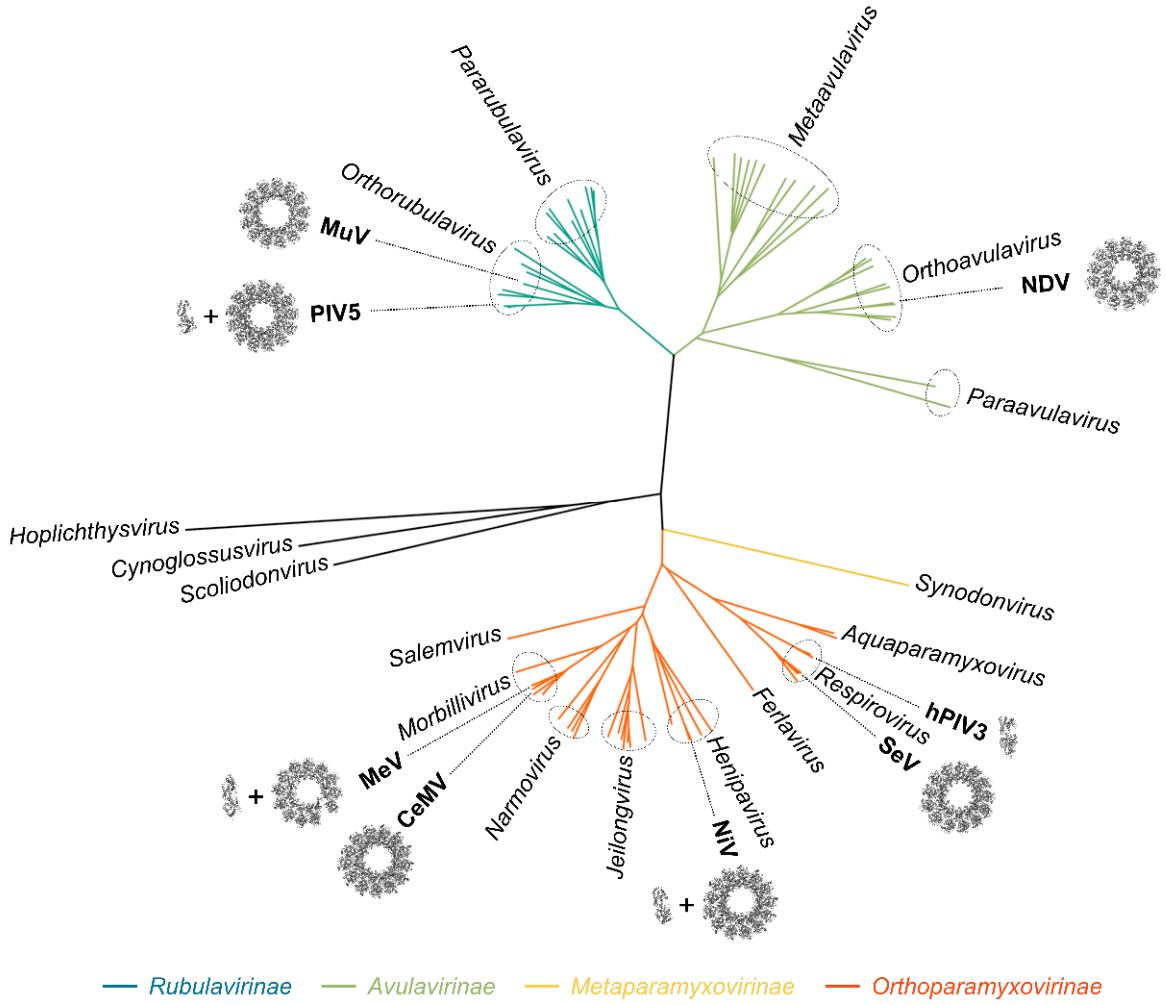

Figure 1. Phylogenetic tree of the *Paramyxoviridae* family. The phylogenetic tree was generated from an alignment of full-length L proteins. One sequence per species was used. The 78 sequences were selected based on the GenBank accession numbers given by the 2020 taxonomy of the International Committee on Taxonomy of Viruses. The names of the genera are indicated in italics. In bold, viruses for which structural data on the N protein is available. Structures of rings or single helical turns of the nucleocapsid-like complexes are shown from a top view (Newcastle disease virus (NDV), reconstructed from PDB: 6JC3; Sendai virus (SeV), reconstructed from PDB: 6M7D; Nipah virus (NiV), PDB: 7NT5; cetacean morbillivirus (CeMV), PDB: 7OI3; measles virus (MeV), PDB: 6h5Q; parainfluenza virus 5 (PIV5), PDB: 4XJN; mumps virus (MuV), PDB: 7EWQ). For human parainfluenza 3 (hPIV3), PIV5, MeV, and NiV, the structures of the N^0-P complexes are shown (hPIV3, PDB: 7EV8; PIV5, PDB: 5WKN; MeV, PDB: 5E4V; NiV, PDB: 4CO6).

The mechanisms used by the polymerase complex to access the encased RNA, progress along the nucleocapsid, and generate new encapsidated products with soluble nucleoprotein monomers are yet to be fully deciphered. However, in the past few years, the atomic structures of the nucleoprotein of a number of paramyxoviruses from different genera have been solved in either assembled [17–23] or non-assembled form [24–27] (Figure 1). Moreover, since the atomic structure of the polymerase complex of parainfluenza virus 5 (PIV5) has been solved, structural information is now available for all the components of the RNA synthesis machinery of paramyxoviruses [28]. Significant progress has also been made on the use of the nucleocapsid as a template, especially on the complex interaction network at play between the nucleoprotein and the phosphoprotein. This review summarizes both structural and functional insights on the nucleocapsid of paramyxoviruses, its assembly, and its role as a template. Models of transcription and replication are proposed.

2. Gene Expression and Genome Replication

2.1. The Viral Genome

The genomes of paramyxoviruses contain a single, bipartite, transcription promoter at the 3′ end, followed by at least six conserved, adjacent genes separated by non-transcribed intergenic regions (Figure 2A) [29–31]. The lengths of the genomes range from 14 to 21 kb and must be multiples of six, the so-called 'rule of six' [32,33]. The conserved genes encode for the nucleoprotein, the phosphoprotein, the matrix protein, the fusion protein, the receptor-binding protein, and the large protein, or polymerase (Figure 2A). While the N, P, and L proteins are the essential components of the viral RNA synthesis machinery, the matrix protein and the two glycoproteins are necessary for the formation of the viral particles and their entry into cells [31].

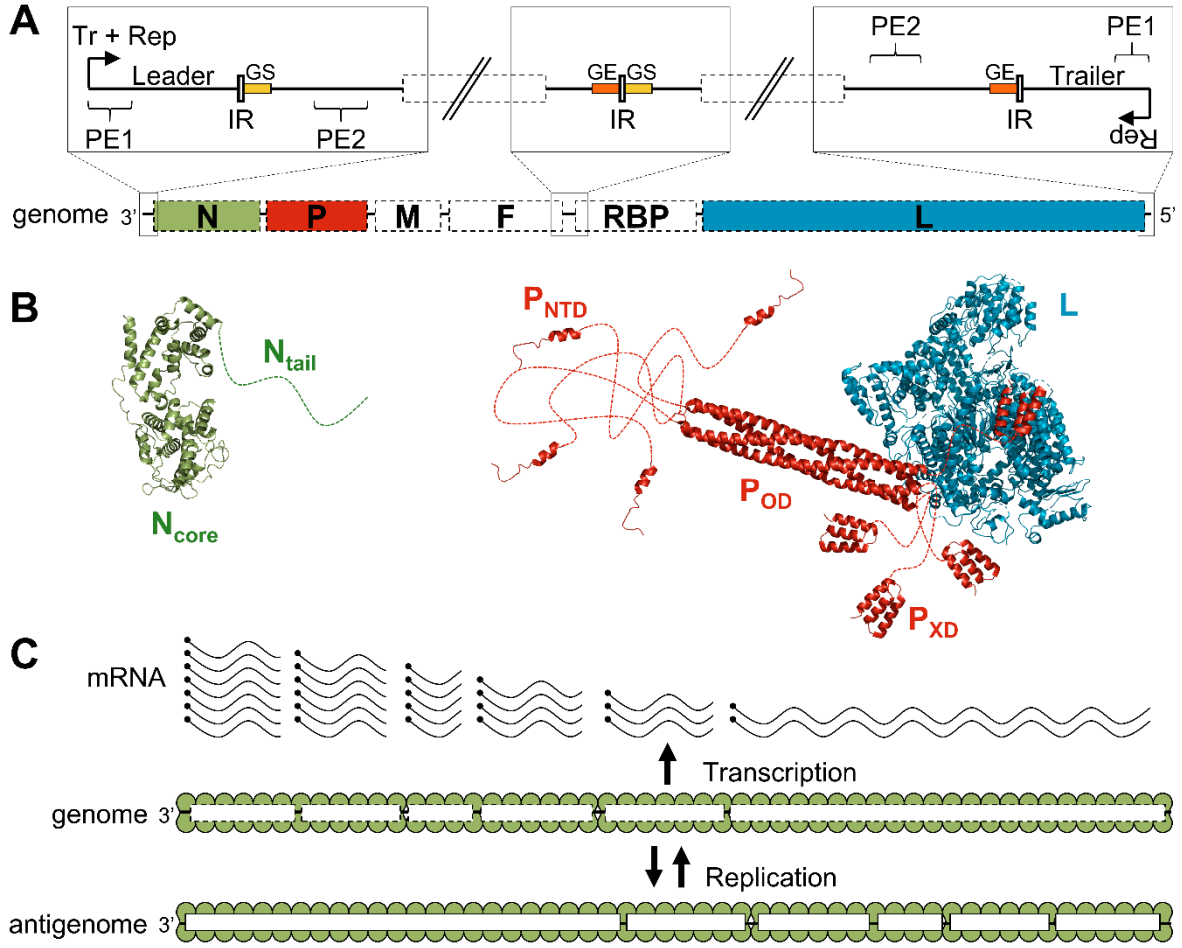

Figure 2. Organization and structure of the components of the RNA synthesis machinery. (**A**) Schematic representation of the viral genome and the regulatory elements. The genome contains at least six conserved adjacent genes separated by intergenic regions (IR). These genes encode for the nucleoprotein (N), the phosphoprotein (P), the matrix protein (M), the fusion protein (F), the receptor-binding protein (RBP), and the large protein (L). The promoters located at the 3′ end of the genome (transcription and replication) and the antigenome (replication only) are bipartite and made of two promoter elements (PE1 and PE2). The transcription of each gene starts on a "gene start" signal (GS, in yellow) and ends on a "gene end" signal (GE, orange). (**B**) Cartoon representation of the structure of the protein components of the RNA synthesis machinery of PIV5 (N, PDB: 4XJN; P_{NTD}, PDB: 5WKN; P_{OD}, P_{XD}, and L, PDB: 6V85). Disordered regions are represented as dotted lines. (**C**) Schematic representation of viral transcription and replication. Encapsidated genomes are transcribed into a gradient of mRNAs. Replication of the genomes requires the production of encapsidated antigenome intermediates.

2.2. Components of the RNA Synthesis Machinery

The nucleoproteins of paramyxoviruses are made of a folded domain (N_{core}) followed by a long intrinsically disordered tail (N_{tail}) [34] (Figure 2B). While N_{core} is responsible for the oligomerization on the RNA and constitutes the main body of the nucleocapsid [35–38], N_{tail} mediates the recruitment of the polymerase complex [34,39,40]. The nucleoproteins self-assemble on the genome due to their affinity for RNA and the interactions between adjacent protomers, as discussed later.

The L protein is a large, multi-domain protein, made of five globular domains linked together by flexible linkers [28,41] (for a review see [42,43]) (Figure 2B). It carries all the enzymatic activities required for transcribing and replicating the genome: RNA synthesis [5,6], mRNA cap addition [44,45], guanine-N-7-methylation of the cap, and ribose 2′O-methylation of the first nucleotide [46,47]. Polyadenylation of the mRNA occurs when the polymerase stutters on a short poly(U) sequence located in a polyadenylation signal [48,49].

The phosphoprotein plays several essential roles: it stabilizes the L protein [7,50–52], recruits the L protein on its template [53], stabilizes the N protein in a monomeric and RNA-free state [54–56], and provides N proteins for the encapsidation of nascent RNA during replication [7,55]. The phosphoprotein's sequence is poorly conserved but its organization in three modules linked by long disordered regions is shared within the viral order [57–62] (Figure 2B). The N-terminal domain (PNTD) binds the nucleoprotein to prevent its self-assembly on RNAs other than viral genomes and antigenomes [55,56]. This interaction forms the N0-P complex, used as a substrate for the encapsidation of the nascent RNA during genome replication [7]. The central domain, or oligomerization domain (POD), forms a long, parallel, coiled-coil tetramer for Sendai virus (SeV) [63], MeV [64,65], NiV [62,66], PIV5 [28], and human parainfluenza virus 3 (hPIV3) [67], but an antiparallel dimer of two parallel coiled-coil dimers for MuV [68,69]. The C-terminal domain, or X domain (PXD), interacts with the nucleoprotein and recruits the polymerase on the nucleocapsid [50,70–75].

2.3. Transcription and Replication

Following fusion of viral and host cell membranes during entry, the polymerase complexes packaged in virions transcribe the viral genes into capped and polyadenylated mRNAs (Figure 2C) [31]. The viral genes are separated by short non-transcribed intergenic regions and contain a gene start (GS) and a gene end (GE) signal at their 3′ and 5′ ends, respectively (Figure 2A). The current model suggests that RNA synthesis starts at the 3′ end of the genome where the polymerase recognizes the transcription promoter. The L protein first synthesizes the leader RNA, a short, uncapped RNA, which is released upon recognition of the first intergenic region. The polymerase then scans the genome to find the first GS signal and re-initiates RNA synthesis. The nascent RNA is capped and methylated by the L protein. Upon recognition of the GE signal, the polymerase adds a poly(A) tail, releases the mRNA, and scans the genome to find the next gene start signal. As the transcription re-initiation is not perfectly efficient, the polymerase generates a decreasing gradient of mRNAs (Figure 2C).

Once the concentration of nucleoproteins reaches a certain threshold, the polymerase can switch from a transcription mode to a replication mode [76,77]. Although the accumulation of N proteins may not be the only trigger, artificially increasing the amount of N proteins advances the onset of replication [77,78]. Initiation of replication occurs when the nascent leader RNA is encapsidated by monomers of N and the polymerase ignores the transcription signals, instead synthesizing a full-length encapsidated copy of the genome (antigenome) [76,79]. This antigenome is then used as a template to generate full-length encapsidated copies of the viral genome (Figure 2C).

Viral transcription and replication take place in the cytoplasm in membraneless inclusion bodies. Viral genomes, together with N, P, and L proteins, are concentrated in these inclusions formed by liquid-liquid phase separations. The disordered regions of the N and

P proteins play a critical role in the formation of these liquid-like structures (for a review, see [80–82]).

Finally, viral transcription and replication are also affected by the phosphorylation status of N and P. Indeed, both N_{tail} [83–85] and the disordered region upstream of P_{OD} [86–94] contain major phosphorylation sites targeted by cellular kinases [95–101]. Although the roles of these phosphorylations are still unclear, data suggest the phosphorylation of some residues can downregulate [85,92,93,100,102] or upregulate RNA synthesis [83,84,91], modify the balance between transcription and replication [103], alter the stability of encapsidated genomes [104], participate in RNA encapsidation [105], tune the interaction between N and P [94], or facilitate the growth of the inclusion bodies [106].

3. Structure of the Nucleocapsid

3.1. Overall Architecture

Nucleocapsids extracted from disrupted virions or infected cells form left-handed, rod-like helical structures with a herringbone appearance under an electron-microscope [107–110] (Figure 3A). The coiling and rigidity of the helix depend on the conditions of the milieu, such as the ionic strength [111]. Indeed, while, at low salt concentration, the nucleocapsids are loose and flexible, and at high ionic strength, the helixes are tight and rigid with a length of about 1 µm and a diameter of 15–20 nm. The flexibility also varies from one virus to another, with the nucleocapsids of MuV being more flexible than the nucleocapsids of MeV, themselves more flexible than the nucleocapsids of SeV or PIV5 [109,112]. Purified intact nucleocapsids from the same virus, or even sections of a single nucleocapsid, can also adopt condensed conformations with different pitches ranging from 5.3 to 6.8 nm for SeV [110], 5.2 to 6.6 nm for MeV [113], or 5.8 to 6.7 nm for MuV [114] (Figure 3C). A smaller pitch correlates with a more rigid and straight helix [112]. In intact MeV particles, the nucleocapsids have a higher pitch (7–8 nm), thus raising the question of whether a preferred pitch exists in physiological conditions and which value it adopts [115]. The average number of N subunits per helical turn is relatively conserved and varies from 12.3 to 13.4 [18,110,113,114]. Removal of the encapsidated RNA from MuV nucleocapsid increases the flexibility of the helix but does not affect its helical conformation, indicating that the nucleocapsid assembly is stable even without RNA [114].

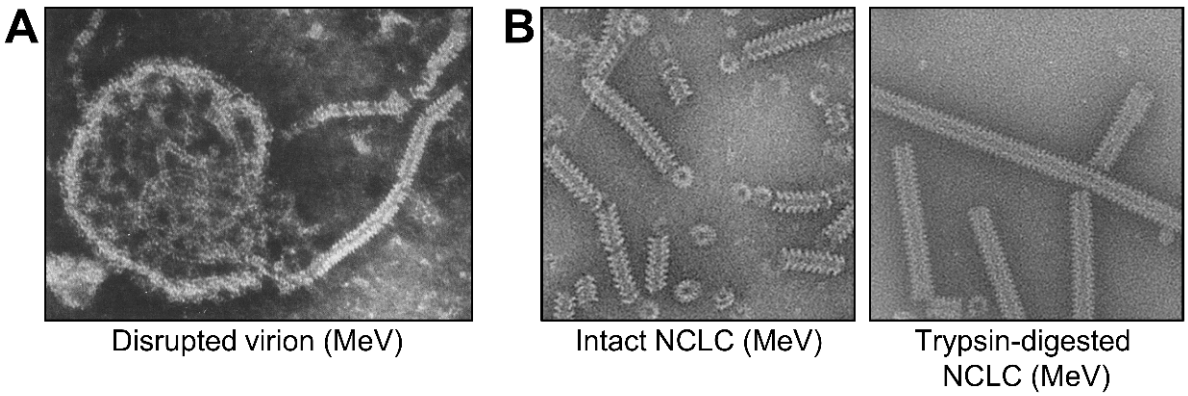

Figure 3. *Cont.*

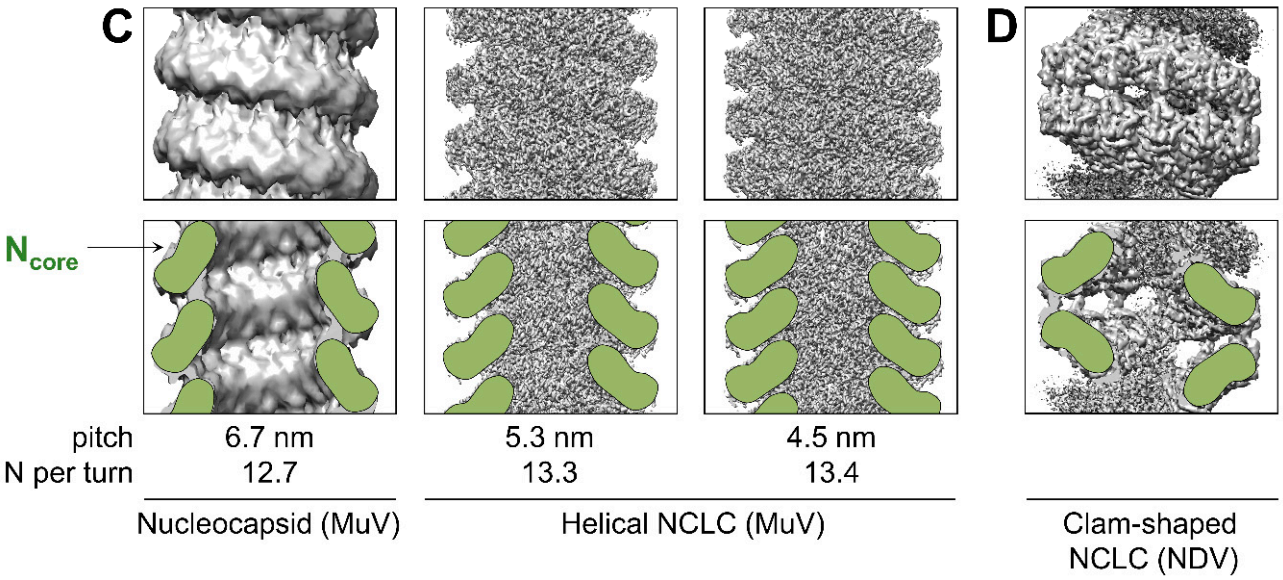

Figure 3. Conformations of nucleocapsids. (**A**) Disrupted measles particle by negative-stain microscopy. Republished with permission of Journal of Virology, from [116]; permission conveyed through Copyright Clearance Center, Inc. (**B**) Intact (left) and trypsin-digested (right) nucleocapsid-like complexes (NCLC) of MeV. Republished with permission of Journal of Virology, from [117]; permission conveyed through Copyright Clearance Center, Inc. (**C**) Top row: density maps of MuV nucleocapsid (left, EMDB: EMD-2630) and MuV NCLC (center, EMBD: EMD-31368; right, EMBD: EMD-31369). Bottom row: cross sections of the density maps shown above with schematic representation of N_{core} in green. The pitch and number of N protomers per helical turn are indicated at the bottom. (**D**) Top: density map of a clam-shaped structure of NDV (EMBD: EMD-9793). Bottom: cross section of the density map shown above with schematic representation of N_{core} in green.

Expression of the nucleoprotein in avian cells [118], mammalian cells [36], insect cells [119], or bacteria [120], induces the formation of nucleocapsid-like complexes (NCLC) containing cellular RNAs. These complexes can form helices [118,121], rings [17,122], or clam-shaped structures [19,21,22] (Figure 3B–D). The last has been observed for NDV, SeV, and NiV, and is made of two helical turns interacting in a back-to-back manner (Figure 3D). The detection of this structure for paramyxoviruses from different genera and its presence in nucleocapsids extracted from NDV and SeV virions, suggests it may be biologically relevant [19,21]. The clam-shaped structure has been proposed to play a role in seeding the assembly of double-headed helices, protecting the 5′ end of the genome from nucleases, and promoting the encapsidation of multiple nucleocapsids per virion [123–125].

3.2. Structure of the Nucleoprotein

The sequence and the organization of N_{core} are well conserved across the *Paramyxoviridae* family, while the sequence and length of N_{tail} vary greatly (Figure 4A). The structure of the N protein in an oligomeric, RNA-bound conformation (i.e., engaged in an NCLC) have been solved for PIV5 [17], MeV [18,20], NDV [19], cetacean morbillivirus (CeMV) [23], NiV [22], SeV [21], and MuV [126], while the structure of N in complex with P_{NTD} (i.e., N^0-P complex) was solved for NiV [24], MeV [25], PIV5 [26], and hPIV3 [27] (Figure 1).

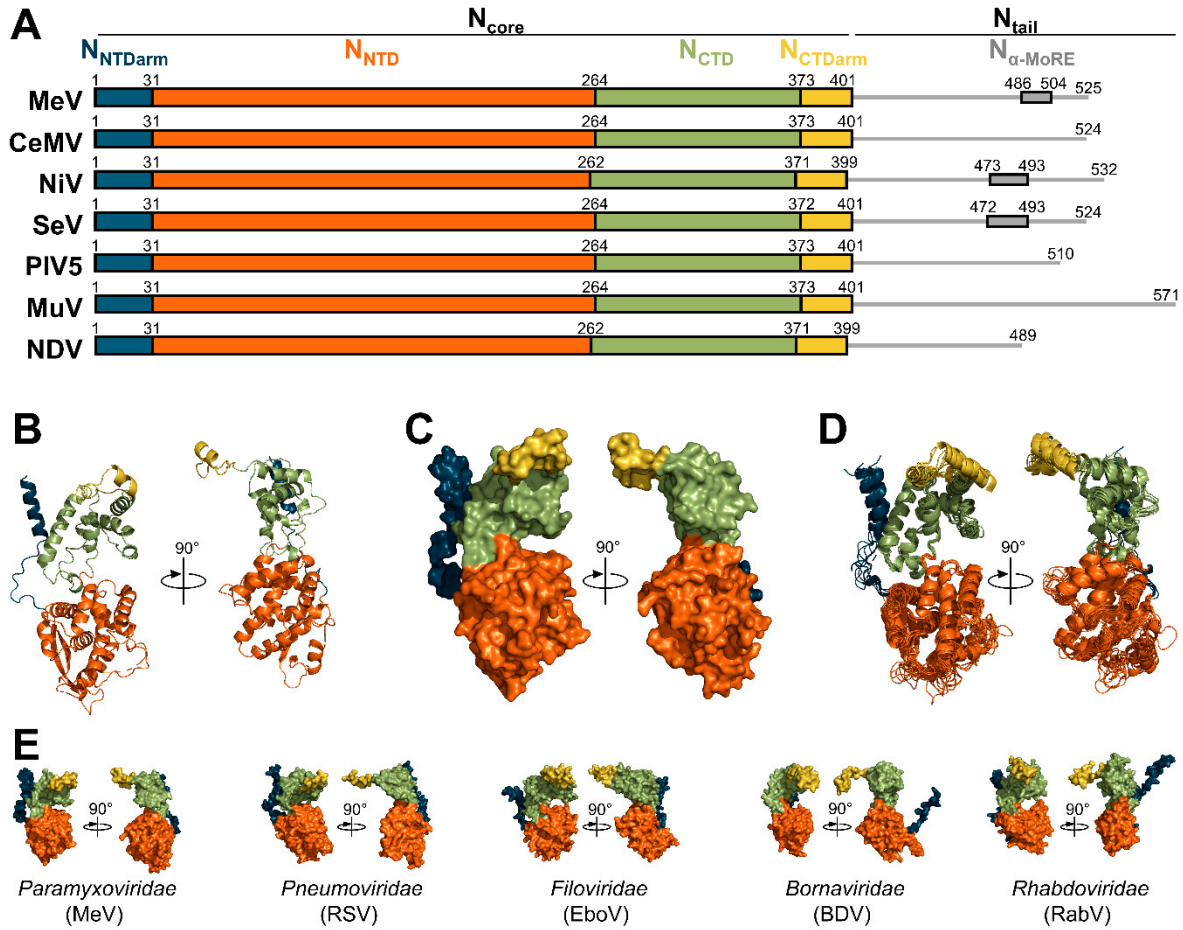

Figure 4. Organization and structure of the nucleoproteins. (**A**) Organization and boundaries of the domains of all nucleoproteins whose structure has been solved. Boundaries of $N_{\alpha\text{-MoRE}}$ are only known for MeV [71,73], NiV [74,127], and SeV [128]. (**B**) Structure of the N protein of MeV in cartoon representations (PDB: 6H5Q). (**C**) Structure of the N protein of MeV in surface representations (PDB: 6H5Q). (**D**) Superimposition of aligned structures of MeV (PDB: 6H5Q), CeMV (PDB: 7OI3), NiV (PDB: 7NT5), SeV (PDB: 6M7D), PIV5 (PDB: 4XJN), MuV (PDB: 7EWQ), and NDV (PDB: 6JC3). (**E**) Surface representations of the structure of the N proteins of MeV (PDB: 6H5Q), respiratory syncytial virus (RSV, PDB: 2WJ8), Ebola virus (EboV, PDB: 5Z9W), Borna disease virus (BDV, PDB: 1N93), and rabies virus (RabV, PDB: 2GTT). All the structures shown in Figure 4 correspond to N proteins observed in their assembled form (i.e., in NCLC).

N_{core} consists of two globular domains, the N-terminal (N_{NTD}) and C-terminal domains (N_{CTD}), which form a positively charged cavity to accommodate the RNA (Figure 4B,C). These domains are preceded and followed by an N-terminal and a C-terminal arm (N_{NTDarm} and N_{CTDarm}) connected by flexible linkers; these arms are responsible for the self-assembly of N protomers onto the RNA. The superposition of the structures of the N proteins of paramyxoviruses shows high conservation of the tertiary and secondary structures (Figure 4D). The global architecture is also well conserved among members of the *Mononegavirales* order, since the N proteins of respiratory syncytial virus (RSV) [129,130] and human metapneumovirus [131] (two pneumoviruses), Ebola virus [132–136] and Marburg virus [137] (two filoviruses), Borna disease virus [138] (a bornavirus), vesicular stomatitis Indiana virus (VSIV) [139] and rabies virus [140] (two rhabdoviruses) have similar structures and modes of self-assembly (for a review see [141]) (Figure 4E).

3.3. Interactions between Protomers

Each N protomer forms tight connections with its neighbors via its two arms protruding on each side of the N protein (Figure 5A). On one side, the N_{NTDarm} of the N_i protomer forms an alpha helix that binds a hydrophobic groove on the back of the N_{CTD} of the N_{i-1}

protomer (Figure 5B(i)). On the other side, the N_{CTDarm} folds in two alpha helixes interacting with the top of the N_{CTD} of the N_{i+1} protomer (Figure 5B(ii)). A third tight connection has been described between an extended loop of the N_{NTD} of the N_i protomer that enters into a hole formed by the N_{NTD} and N_{NTDarm} of the N_{i+1} protomer (Figure 5B(iii)) [21,126]. In addition to these interactions, there are large contact areas between adjacent protomers with numerous additional bonds [23].

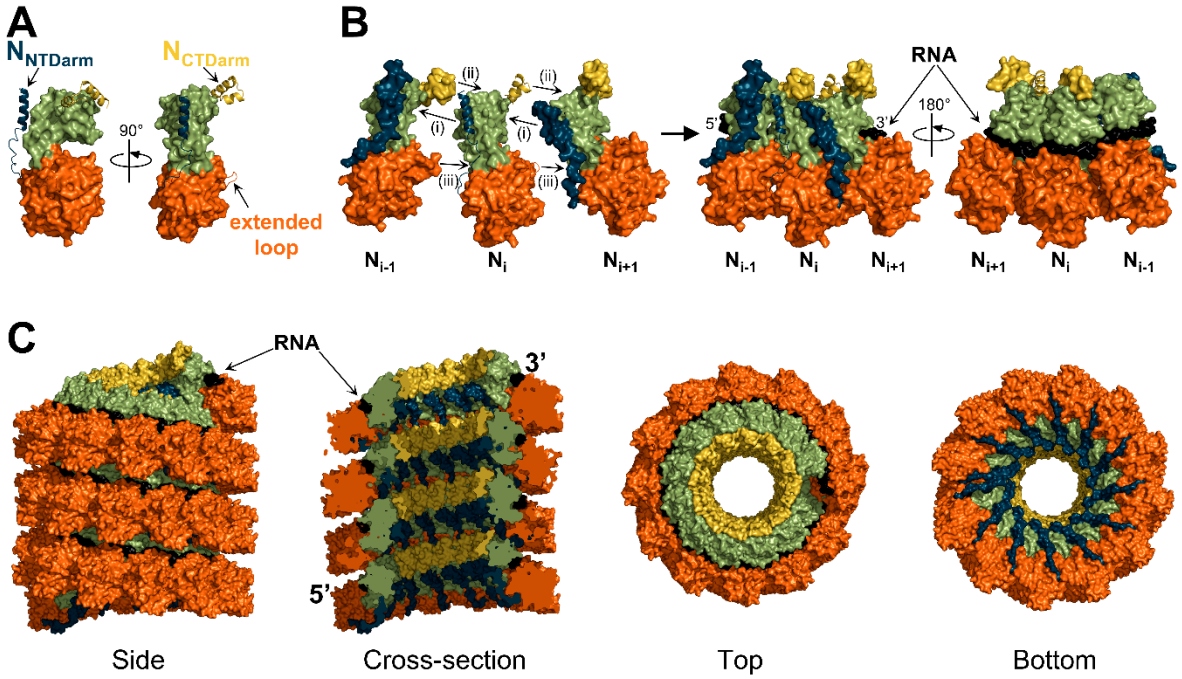

Figure 5. Mode of assembly. (**A**) Structure of the nucleoprotein of PIV5 shown in surface representation, except for the N_{NTDarm}, N_{CTDarm}, and extended loop, which are shown in cartoon representation (PDB: 4XJN). (**B**) Surface representation of three N protomers with the N_{NTDarm}, N_{CTDarm}, and extended loop of the N_i protomer shown in cartoon representation. The RNA is shown in black. (**C**) Surface representation of a nucleocapsid-like complex of MeV shown with four different views (reconstituted from PDB: 6H5Q). Color code is the same as in Figure 4.

These N-N interactions curve the N oligomer so that the RNA is exposed on the outside of the helix (or ring) and all the tight inter-protomer connections are hidden inside the helix (Figure 5C) [17,18,117]. This conformation is similar to that observed in the nucleocapsids of filoviruses [134] and pneumoviruses [130], but opposite to the one found in rhabdoviruses [142,143] where the RNA is located in the interior of the helical nucleocapsid.

3.4. Interactions with RNA

The genomic RNA is inserted in a cavity formed by the N_{NTD} and the N_{CTD} (Figure 6A,B). Each N protomer binds six nucleotides in agreement with the rule of six [17,18]. The RNA is mainly stabilized by interactions between positively charged residues and the RNA backbone, thus explaining the low sequence specificity of encapsidation (Figure 6A). The RNA adopts a regular conformation with a three-base stack oriented outwards to the solvent (bases "out") and the following three-base stack facing toward the protein (bases "in") (Figure 6B).

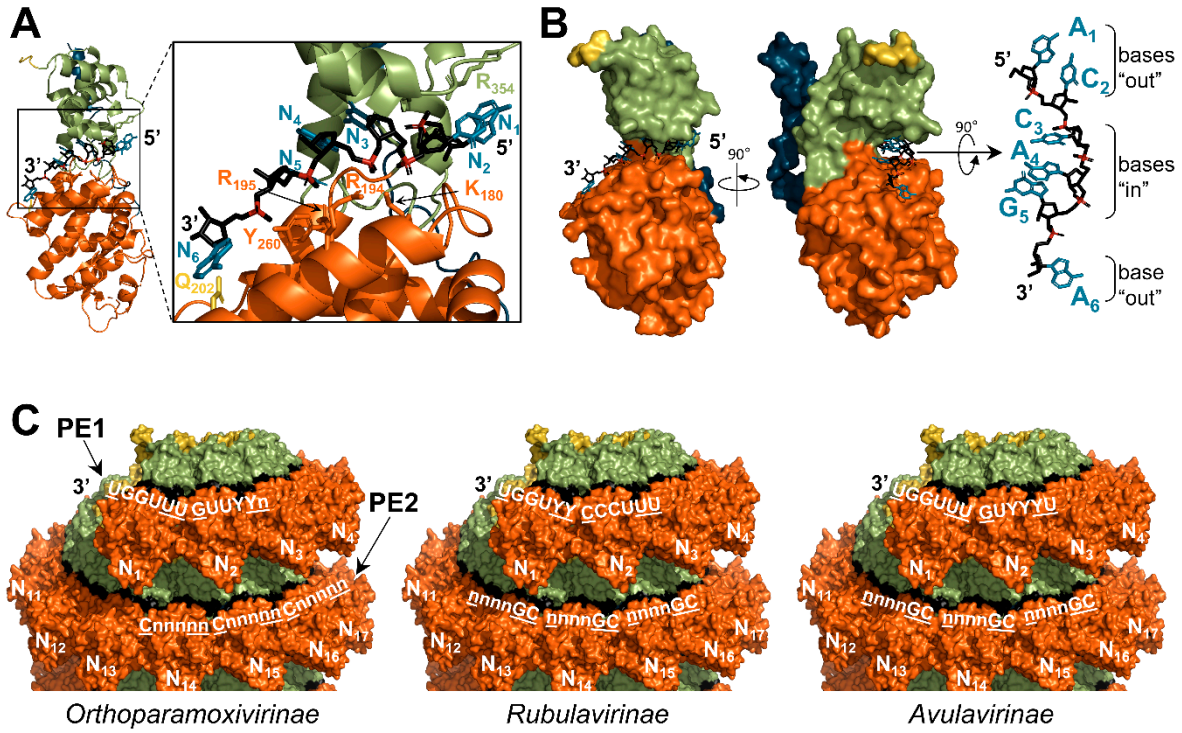

Figure 6. Position of the RNA. (**A**) Cartoon representation of MeV nucleoprotein bound to the first six nucleotides of the genome (5′ end) (PDB: 6H5S). The RNA and the residues implicated in the binding to the RNA are represented with sticks. The bases of the RNA are shown in blue, the backbone in black, and the phosphates in red. Residue Q202 is shown in yellow. (**B**) Same as (**A**) with the nucleoprotein in surface representation. (**C**) NCLCs of CeMV are shown in surface representation (reconstitution of the helix from PDB: 7OI3). For each subfamily, the consensus sequences of the promoter elements (PE1 and PE2) are shown in white. Well-conserved nucleotides are in capital letters. Bases in "out" positions are underlined. For N, same color code as in Figure 4.

Using recombinant N proteins fused to a cleavable P_{NTD}, NCLCs were generated in vitro after cleavage of the P_{NTD} and incubation with either a six-nucleotide-long poly(A) RNA or an RNA corresponding to the first six nucleotides of the viral genome [20,23]. For both MeV and CeMV, NCLCs adopt a helical conformation with the RNA hexamer in the same phase register. These structures suggest that the first two nucleotides of the viral genome point toward the solvent and that the 3′ end of the genome is accessible to the viral polymerase (Figure 6B). This register is in agreement with data showing that cytidines at positions 1 and 6, which are both in "out" positions, are more sensitive to chemical modifications [144].

Paramyxoviruses have bipartite promoters [145–148] (for a review see [30]). The first promoter element (PE1) contains at least the first twelve nucleotides of the genome (Figure 2A). The second promoter element (PE2) is composed of three successive hexamer sequences: 3′-CNNNNN-5′ located at positions 14 to 16 (in the hexamer register) for orthoparamyxoviruses [146], and 3′-NNNNCG-5′ at position 13 to 15 for rubulaviruses [147] and avulaviruses [148]. According to the RNA register described for MeV and the average of 13 N per turn for native nucleocapsids, PE2 is located in the successive turn of the helical nucleocapsid just under PE1 in the helical conformation of the nucleocapsid (Figure 6C). Moreover, the conserved nucleotides of the two types of PE2 are facing the solvent, thus reinforcing the idea that these bases could be sensed by the polymerase complex and participate in promoting RNA synthesis.

The side chain of the residue Q202 of the nucleoproteins of PIV5 and MeV interacts with the base of the nucleotide in position six, and thus the first nucleotide of the promoter [17,20] (Figure 6A). In a cell-based minigenome assay, mutation Q202A of the N protein of human parainfluenza virus 2 allows the transcription and replication of the

minigenome, irrespectively of whether its length is a multiple of six and the presence of the PE2 element [149,150]. The authors suggest that residue Q202 may stabilize the first nucleotide of the genome, thus inhibiting the initiation of RNA synthesis by the viral polymerase. PE2 would then promote RNA synthesis initiation by stabilizing the polymerase complex on the promoter. Since the function of PE2 depends on its phase register, the requirement of PE2 would ensure the conservation of the rule of six [149,150].

In addition to its impact on the promoters, the phase of the RNA bases also affects the transcription signals. Indeed, during transcription, the P messenger RNA of paramyxoviruses can be edited by the viral polymerase which adds one or several extra G residues by stuttering along a short stretch of C residues [151]. Incremental modifications of the phase register of the editing site modify the efficiency of the editing and the number of residues added [144]. Moreover, within each genus, the gene start signals are found in a few preferred phases, suggesting the phasing of the gene start signal may also affect the efficiency of the re-initiation of transcription at gene junctions [33]. Overall, these results show that the imprint of the N protomers on the RNA influences how the viral polymerase uses its template.

3.5. Position and Influence of N_{tail} within the Nucleocapsid

N_{tail} belongs to the group of pre-molten globules within the class of intrinsically disordered proteins [34,57,59]. Although N_{core} is sufficient to generate the helical core of the nucleocapsid [35,36,38], N_{tail} influences the conformation of the helix. Indeed, treatment of the nucleocapsid or NCLC by trypsin cleaves off N_{tail}, reduces the pitch, and tightens the helix [21,34,113,117,121] (Figure 3B). Moreover, while the expression of the full-length N protein of MuV generates NCLCs in a ring conformation, the cleavage of N_{tail} generates helical structures [126].

In agreement with its disordered nature, N_{tail} is not visible by electron microscopy [34,113,126]. Nuclear magnetic resonance spectroscopy and small-angle scattering showed that N_{tail} escapes from the nucleocapsid core toward the exterior between two helical turns [152] (Figure 7A,B), in agreement with the location of epitopes recognized by antibodies targeting N_{tail} [153]. While the first 50 residues of N_{tail} are spatially constrained by the helical turns of the nucleocapsid core, the C-terminal residues have high angular freedom [75,127,152]. This model is further supported by the recently solved structure of the NCLCs formed by SeV N proteins [21]. After cleavage of most of N_{tail}, the nucleocapsids were found to become more rigid and allowed a resolution of 2.9 Å. The atomic model was reconstituted up to residue 414, thus including the first thirteen residues of the tail (aa 402-414). The residues bind the surface of N_{CTD} and point toward the exterior of the nucleocapsid core (Figure 7A).

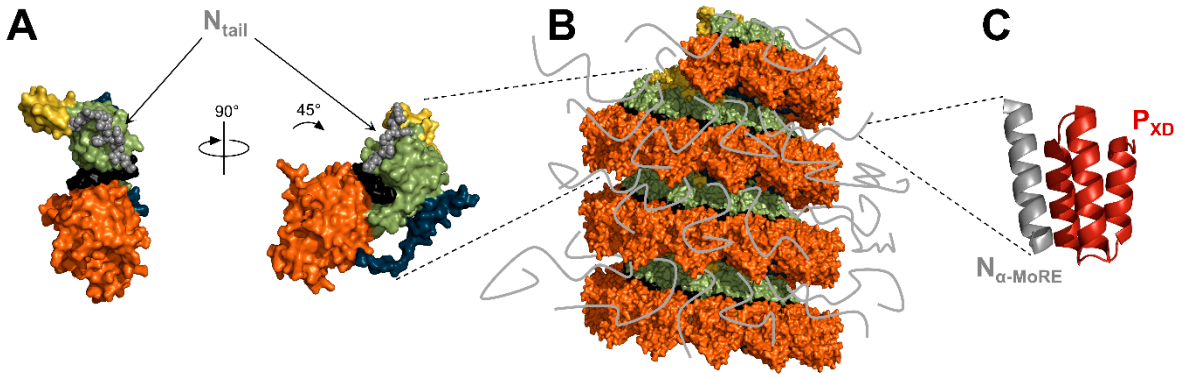

Figure 7. Structure and position of N_{tail}. (**A**) Structure of the nucleoprotein of SeV in surface representation with the residues of N_{tail} shown with spheres (PDB: 6M7D). (**B**) Surface representation of the nucleocapsid-like complex of CeMV with the N_{tail} represented as grey lines (reconstitution from PDB: 7OI3). (**C**) Structure of MeV P_{XD} in complex with $N_{\alpha\text{-MoRE}}$ (PDB: 1T6O). For N, the color code is the same as in Figure 4.

N_{tail} is thought to mediate the contact between the nucleocapsid and its environment. While N_{tail} is not required for the encapsidation of the RNA, it is essential for RNA synthesis [37,154]. Indeed, N_{tail} contains an α-helical molecular recognition element (α-MoRE) which folds upon binding to the C-terminal domain of the phosphoprotein (P_{XD}) and thus participates in the recruitment of the polymerase complex on its template [39,40,71,73–75,127,128,153,155–157] (Figure 7C). In addition to its interaction with P_{XD}, N_{tail} also binds the matrix protein, thus promoting the packaging of the nucleocapsids into viral particles [158–162]. N_{tail} also mediates the interaction with several cellular factors [61], including heat shock protein 70 (hsp70) [154,163,164] and peroxiredoxin 1 [165].

4. Formation of the Nucleocapsid

4.1. Structure of the N^0-P Complex

The N-terminal domain of the phosphoprotein interacts with the monomeric, RNA-free form of the N protein (referred to as N^0), thus forming the so-called N^0-P complex [55,166]. This interaction prevents the formation of NCLCs on cellular RNAs and recruits the N proteins to the encapsidation site where N^0-P complexes are used as the substrate for the encapsidation of genomes and antigenomes [7,55,56].

The first 50 residues of P (herein referred to as P_{NTD}) of paramyxoviruses contain a conserved α-MoRE [57,59,62,167] that adopts an alpha-helical structure upon binding to N_{core} (Figure 8). The structures of the N^0-P_{NTD} complex of NiV [24], MeV [25], PIV5 [26], and hPIV3 [27] were solved by X-ray crystallography (Figure 8A–D). To crystallize the complex in a monomeric and RNA-free state, the N_{NTDarm} and N_{CTDarm} were removed (with the exception of MeV in which the N_{CTDarm} was included). For all three viruses, P_{NTD} binds to N_{CTD} in the groove occupied by the N_{NTDarm} of the adjacent N_{i+1} protomer in the nucleocapsid conformation (Figure 8B). The interactions between the groove and the P_{NTD} or the N_{NTDarm} are both of hydrophobic nature. For MeV and NiV, the first alpha-helix is followed by a second alpha-helix segment that binds the top of the N_{CTD} in place of the N_{CTDarm} of the adjacent N_{i-1} protomer (Figure 8B). Contrary to MeV, hPIV3, and NiV, the P_{NTD} of PIV5 extends on its N-terminus and reaches the RNA cavity, potentially directly inhibiting binding to the RNA (Figure 8C). Inhibition of the binding of the arms of the adjacent N protomers by P_{NTD} is a conserved feature among mononegaviruses [131,137,168–172].

For MeV, NiV, and PIV5, the structures of both the RNA-free N_{core} in complex with P_{NTD} and the RNA-bound N_{core} engaged in an NCLC (N^{NUC}) have been solved. The overall architecture of N_{core} is conserved between the N^0 conformation (or "open" conformation) and the N^{NUC} conformation (or "closed" conformation) (Figure 8D). Although individually the N_{NTD} and N_{CTD} have very similar structures, their relative orientation differs (Figure 8D–F). Indeed, the kinked alpha-helix located between the N_{NTD} and the N_{CTD} acts as a hinge and allows the rotation of the N_{CTD} (Figure 8F). This rotation finalizes the formation of the RNA cavity. While NiV P_{NTD} has been suggested to maintain the N protein in the N^0 conformation by rigidifying the structure [24], modeling and molecular simulations suggest that the PIV5 N protein preferably adopts the N^0 conformation in the absence of ligand (P_{NTD} or RNA) [26]. The interactions between the RNA backbone and residues from both the N_{NTD} and N_{CTD} most likely participate in the stabilization of the N^{NUC} conformation, even in the absence of adjacent protomers.

In addition to P_{NTD}, another ultra-weak interaction was detected between N_{core} and a fragment of the long, disordered region of P located between P_{NTD} and P_{OD} [173]. This fragment contains a short peptide (δ) with no apparent secondary structure and a transient short alpha-helix (α4), which both interact with the bottom of N_{NTD} (Figure 8G). The sequence of α4 has some level of conservation among morbilliviruses and henipaviruses, and the introduction of mutations in this sequence inhibits gene expression in a minigenome assay. The homologous sequence in the NiV P protein also adopts a transient alpha-helix structure in solution [62,174]. Thus, this ultra-weak interaction may be conserved and essential for maintaining the N protein in the N^0 state [173]. The interaction between the α-MoRE of N_{tail} ($N_{α\text{-}MoRE}$) and P_{XD} may also further stabilize the N^0-P complex [175].

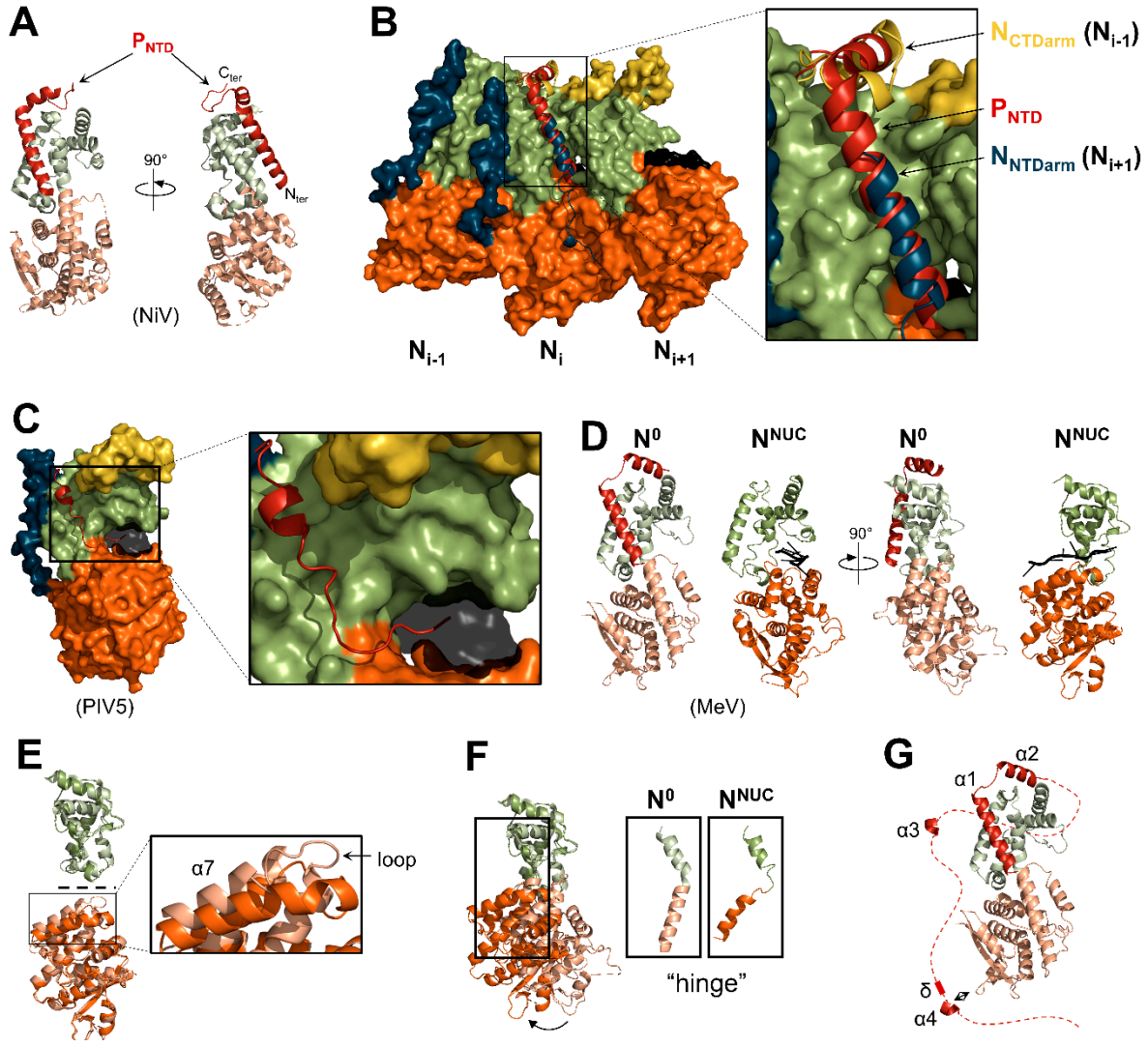

Figure 8. Structure of the N^0-P complex. (**A**) Structure of the N^0-P complex of NiV (PDB: 4CO6). The N_{NTD} and the N_{CTD} are in pale orange and pale green, respectively. (**B**) Superimposition of the structure of three N protomers of NiV NLPC (PDB: 7NT5) with NiV N^0-P (PDB: 4CO6). The N_{CTD} of the N^0-P complex was aligned onto the N_{CTD} of the N_i promoter. The N protomers are presented in surface representation, while the N_{NTDarm}, N_{CTDarm}, and the extended loop of the N_i protomer are shown in cartoon representation. P_{NTD} is shown in cartoon representation. (**C**) Structure of the N^0-P complex of PIV5 with P_{NTD} in cartoon representation (PDB: 5WKN). The RNA is shown as a transparent black surface. (**D**) Side-by-side comparison of the structures of the N^0-P complex (PDB: 5E4V) and of an N protomer of the NCLC of MeV (PDB: 6H5Q) (N_{NTDarm} and N_{CTDarm} are not shown). The N_{NTD} and the N_{CTD} of N^0 are in pale orange and pale green, respectively. (**E**) Superimposition of the N_{CTD} (top) and of the N_{NTD} (bottom) of the N^0-P complex and of an N protomer of the NCLC of MeV. (**F**) Superimposition of the structures of MeV N^0 and N^{NUC} (N_{NTDarm} and N_{CTDarm} are not shown). The structures are aligned based on their N_{CTD}. (**G**) Structure of the MeV N^0-P complex with the disordered region downstream P_{NTD} shown as a dotted line. The transient alpha-helices (α3 and α4) are shown in cartoon representation.

4.2. Encapsidation of the RNA

The fusion of full-length N protein (or N_{core}) to a cleavable P_{NTD} allows the production of soluble N^0-P complexes [20,23,176]. Incubation of these complexes with RNA triggers the formation of NCLCs in vitro. This experimental setup revealed that the encapsidation of the RNA is sequence-specific and that the N protein of MeV preferably encapsidates a poly(A) hexamer (but not poly(U)), as well as an RNA corresponding to the first six nucleotides of the genome. Similar specificity was observed for other mononegaviruses, suggesting that the N protein has a higher affinity for poly(A) RNA and the first nucleotides

of the corresponding genome [177–180]. The formation of long helical NCLCs from short RNA hexamers indicates that a continuous RNA molecule is not required for the assembly of N proteins. The kinetics of the encapsidation was analyzed by real-time nuclear magnetic resonance and fluorescence spectroscopy and revealed a two-step mechanism. The first step is rapid and could correspond to the binding of N monomers to the RNA, while the second step consists of the assembly of RNA-bound N proteins [176].

Finally, the local concentration of N^0-P complexes seems critical to efficient encapsidation of the RNA and generation of NCLCs. Indeed, the formation of droplets formed by liquid-liquid phase separation increases both the local concentration of N^0-P complexes and the rate of formation of NCLCs in vitro [181]. For VSIV (*Rhabdoviridae* family), although dispensable [182], P_{OD} enhances genome replication possibly by increasing the local concentration of N^0 at the site of encapsidation [183].

5. The Nucleocapsid as a Template

Unlike the distantly related members of the *Articulavirales* and *Bunyavirales* orders for which the polymerase can directly bind the extremity of the viral genomes, the viral polymerase of mononegaviruses cannot interact with its nucleocapsid template without its cofactor P [43]. Moreover, the genomes of mononegaviruses are deeply encased in helical nucleocapsids, thus raising the question of how the polymerase accesses the RNA.

5.1. Recruitment and Progression of the Polymerase Complex

Since P_{XD} mediates the interaction of L with the nucleocapsid and the polymerase complex is made of the L protein and a tetramer of P proteins, the polymerase complex possesses four potential nucleocapsid-binding sites. This architecture is the basis of the so-called "cartwheeling" model in which the polymerase complex progresses on its template due to cycles of association/dissociation between P_{XD} and the nucleocapsid [184,185].

The P_{XD} of paramyxoviruses adopts a three-helix bundle structure [71–73,75,186,187]. P_{XD} binds to the α-MoRE of N_{tail} [73–75,127,128], the L protein [28,188,189], and N_{core} [68,114,190,191] (Figure 9). P_{XD} has a prism-like shape with three faces: α1 + α2 form face 1 (F1), α2 + α3 form face 2 (F2), and α3 + α1 form face 3 (F3) (Figure 9A). Each interaction is mediated by a different face, with $N_{\alpha\text{-MoRE}}$ interacting with F2 [73], the L protein with F3 [28,189], and N_{core} with F1 [191] (Figure 9).

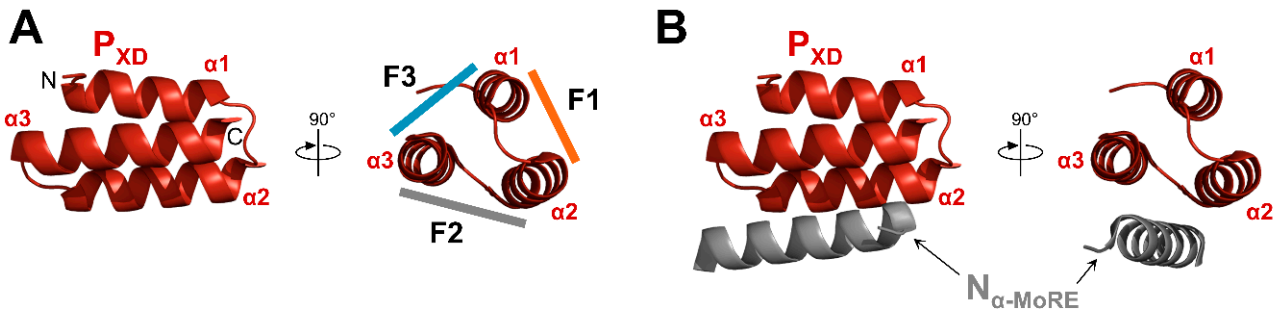

Figure 9. *Cont.*

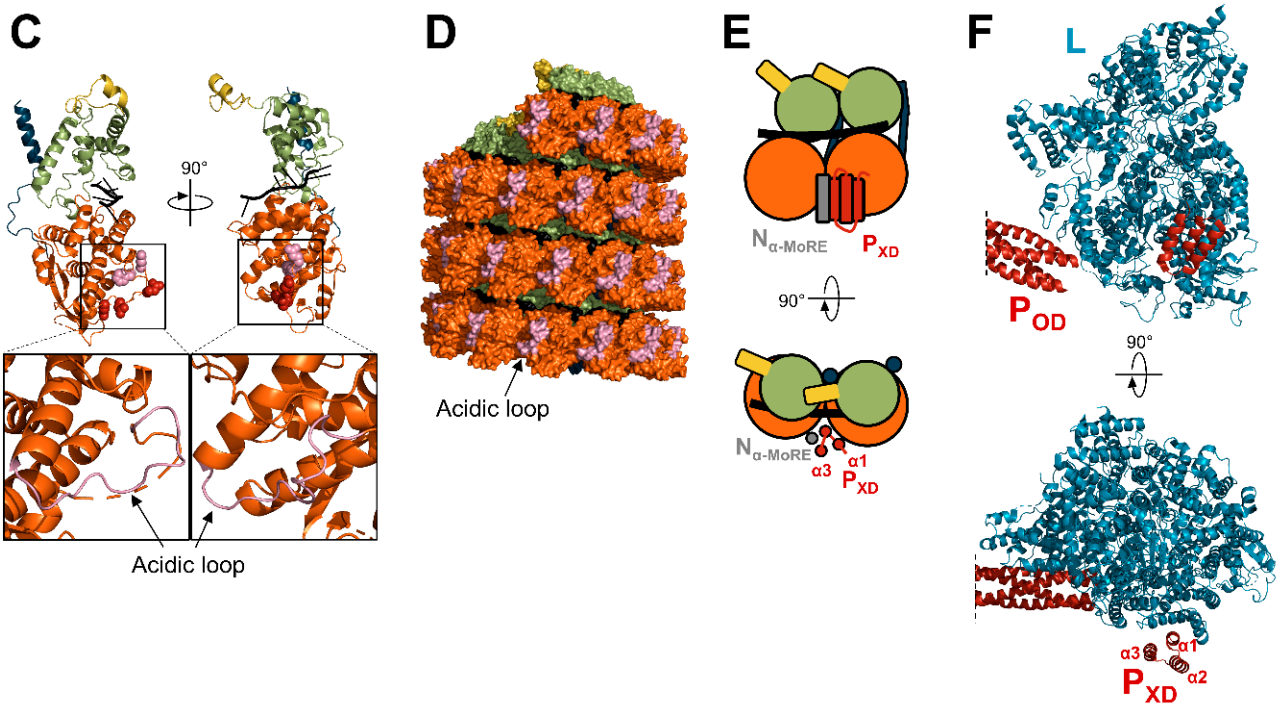

Figure 9. Interaction network of P_{XD}. (**A**) Structure of MeV P_{XD} (PDB: 1T6O). The three faces of the "prism" are indicated (F1, F2, F3). F1, F2, and F3 are shown with a color code corresponding to the color used to draw the protein partner. (**B**) Structure of MeV P_{XD} in complex with $N_{\alpha\text{-MoRE}}$ (PDB: 1T6O). (**C**) Structure of a protomer of MeV N, as observed in the NCLC (PDB: 6H5Q) with the RNA shown in black. Amino acids shown as red spheres correspond to CDV N residues that once mutated restore the growth of a recombinant CDV bearing deletions in the N_{CDR} [191]. The amino acids corresponding to the residues of NiV identified as important for the interaction with P_{XD} are shown as pink spheres [192]. Bottom: enlargements of the N_{NTD} with the acidic loop shown in pink. (**D**) Surface representation of a nucleocapsid-like complex of MeV (reconstituted from PDB: 6H5Q) with the acidic loop shown in pink. (**E**) Schematic representation of two adjacent N protomers bound to P_{XD} in complex with $N_{\alpha\text{-MoRE}}$. (**F**) Structure of the polymerase complex of PIV5 (PDB: 6V85). For panels (**C**–**E**), N protomers are colored according to the color code in Figure 4.

The interaction of P_{XD} with $N_{\alpha\text{-MoRE}}$ is weak, with a constant of dissociation (K_D) in the µM range [74,128,157,193]. While the disordered $N_{\alpha\text{-MoRE}}$ folds into an alpha-helix upon binding to P_{XD}, the flanking regions of N_{tail} remain disordered [74,75,127,187,194–197]. This phenomenon, called fuzziness [198], affects the interaction between N_{tail} and its partners. Indeed, the long-disordered region upstream of $N_{\alpha\text{-MoRE}}$ slows the disorder-to-order transition of $N_{\alpha\text{-MoRE}}$ upon binding to P_{XD} [199,200]. Accordingly, the deletion of the disordered region upstream MeV, NiV, and HeV $N_{\alpha\text{-MoRE}}$ increases the affinity for P_{XD} (and also HSP70 for MeV) [199]. The dampening effect of the disordered regions does not directly depend on the sequence, but rather on a combination of length and disorder. Although not directly involved, the poorly conserved disordered region of N_{tail} upstream the $N_{\alpha\text{-MoRE}}$ affects the interaction with P_{XD} [199–201].

The low affinity between P_{XD} and $N_{\alpha\text{-MoRE}}$ permits efficient progression of the polymerase complex on the nucleocapsid. Indeed, modifications of the binding strength between MeV P_{XD} and $N_{\alpha\text{-MoRE}}$ alter the activity of the polymerase [202–204]. Indeed, there is a positive correlation between the $P_{XD}/N_{\alpha\text{-MoRE}}$ interaction strength and the efficiency of the re-initiation of the transcription at gene junctions [204] (Figure 2A). This effect is further enhanced when the polymerase crosses long non-transcribed intergenic regions, suggesting the $P_{XD}/N_{\alpha\text{-MoRE}}$ interaction keeps the polymerase in an active state when crossing the gap between transcription units.

Although the $P_{XD}/N_{\alpha\text{-MoRE}}$ interaction regulates the activity of the polymerase, it is not strictly required for RNA synthesis. Indeed, while the truncation of MeV N from

$N_{\alpha\text{-MoRE}}$ to its C-terminus abrogates gene expression in a minigenome assay, further deletion of the 43 upstream residues restores activity [205] (Figure 10). This suggests that the central disordered region (N_{CDR}) upstream of the $N_{\alpha\text{-MoRE}}$ has a negative effect on the activity of the polymerase and the binding of P_{XD} to $N_{\alpha\text{-MoRE}}$ counteracts this effect. Accordingly, deletions in the N_{CDR} of CDV and NiV increase activity [206], and when MeV $N_{\alpha\text{-MoRE}}$ is relocated to a variable region of N_{NTD}, removing N_{CDR} enhances gene expression [207] (Figure 10). However, a recombinant MeV harboring $N_{\alpha\text{-MoRE}}$ on N_{core} and devoid of N_{CDR} produces more polycistronic mRNAs. Similarly, two recombinant CDV with deletions in N_{CDR} produce more polycistronic mRNA and show an altered RNA synthesis balance with enhanced transcription over replication [206]. Therefore, the central disordered region of N_{tail} inhibits RNA synthesis, and P_{XD} counterbalances this negative effect. This interplay would finely tune the polymerase's activity and ensure the quality of the generated mRNAs by improving the recognition of the signals at the intergenic junctions.

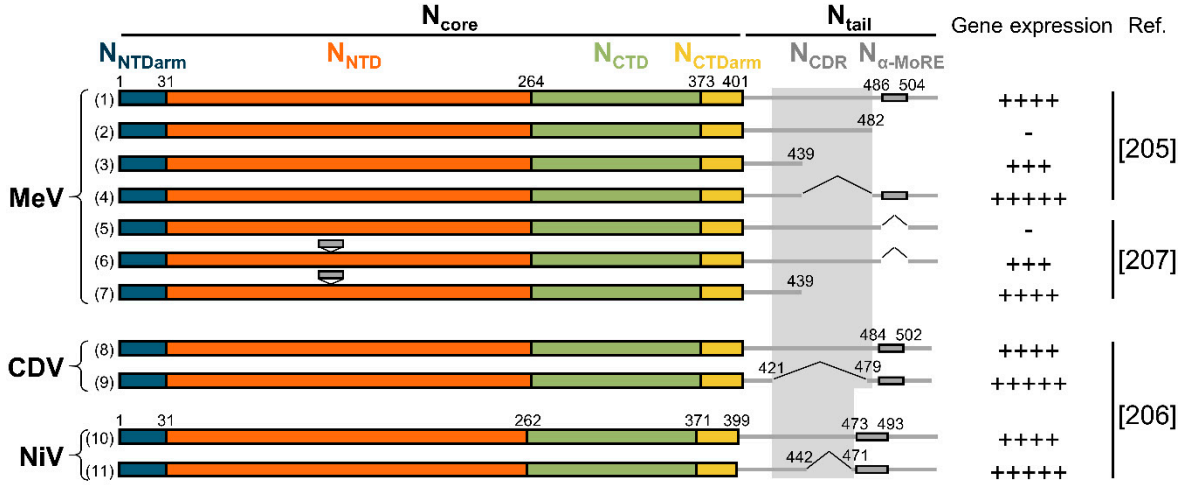

Figure 10. Summary of experimental data on the effect of N_{tail} on the polymerase's activity. Schematic representation of recombinant N proteins analyzed in minigenome assays. The levels of gene expression are normalized to the level of the wild-type protein (first protein of each set). Activity levels: 0–10%: "-"; 50–75%: "+++"; 75–100%: "++++"; >100%: "+++++". For mutants (6) and (7) $N_{\alpha\text{-MoRE}}$ is inserted in a loop of N_{NTD} at residue 138. Mutants (4), (5), (6), (9), and (11) contain internal deletion shown with a "^". Activity levels are inferred from the references indicated on the right.

In addition to interacting with the α-MoRE, P_{XD} of CDV was also shown to directly interact with N_{core} [191]. This interaction is mediated by an acidic loop of N_{NTD} (residues 146 to 161) and requires the presence of $N_{\alpha\text{-MoRE}}$ in complex with P_{XD} (Figure 9C–E). Accordingly, mutations in the homologous region of NiV N_{core} were previously shown to inhibit the P-N interaction [192]. After several passages of a recombinant CDV expressing a N_{tail} with a large deletion in N_{CDR}, compensatory mutations appeared in P_{XD} and N_{NTD} that decreased the affinity between the two domains. Thus, N_{CDR} may inhibit the interaction of P_{XD} with N_{core}. Modeling and molecular docking predict that the $P_{XD}/N_{\alpha\text{-MoRE}}$ complex binds between two N protomers. On one side the F1 of P_{XD} binds to the acidic loop of one protomer and on the other side, $N_{\alpha\text{-MoRE}}$ interacts with a different loop (residues 133 to 142) of the N_{NTD} of the other protomer (Figure 9D,E). The requirement of $N_{\alpha\text{-MoRE}}$ for this interaction suggests P_{XD} first binds $N_{\alpha\text{-MoRE}}$ and then N_{core}. A similar interaction with the acidic loop may explain the singular behavior of MuV P_{XD}, which can bind N_{core} in the absence of N_{tail} [68,190]. This atypical phenotype may be linked to the lower stability of the MuV P_{XD} tertiary structure in solution and to a folding-upon-binding mechanism [186,190]. The binding of CDV P_{XD} to N_{NTD} also agrees well with the density map of MuV nucleocapsids bound to P_{XD} [114]. The P protein of the respiratory syncytial virus (*Pneumoviridae* family) also binds the nucleocapsid on the same location on N_{NTD},

suggesting an ancestral mode of interaction between the polymerase complex and its template [191,208,209].

P binds the L protein via the C-terminal part of the P_{OD} and the third face of the P_{XD} of one P protomer [28,188,189] (Figure 9F). Using different combinations of mutants in a minigenome assay, it was shown that at least one P_{XD} of the tetramer must have the ability to bind the L protein and one different P_{XD} must be able to bind $N_{\alpha\text{-MoRE}}$ [189]. The P_{XD} that binds L does not have to be able to bind $N_{\alpha\text{-MoRE}}$ and it is unclear whether P_{XD} can simultaneously bind L and $N_{\alpha\text{-MoRE}}$. It is also unknown whether the interaction between L and P_{XD} is stable or undergoes rounds of association/dissociation during RNA synthesis.

Of note, some cellular factors influence the progression of the polymerase complex. For instance, hsp70 [163] and peroxiredoxin 1 [165] both compete with P_{XD} for the binding to N_{tail} and enhance RNA synthesis.

Taken together, these results show that P_{XD} is at the core of an interaction network, which is more complex than initially anticipated. P_{XD} participates in a finely regulated dance allowing the progression of the polymerase complex onto the nucleocapsid and the optimal recognition of the transcription signals.

5.2. Access to the RNA

The viral genome is encased between the N_{NTD} and N_{CTD} of each N protomers, with only half of its bases facing the solvent. Thus, copying of the genome requires significant conformational rearrangements to allow the RNA to reach the catalytic site of the polymerase.

First, in the straight helical conformation of purified nucleocapsids, the RNA is covered by the N protomers of the adjacent helical turn, leaving an insufficient empty space above the RNA to accommodate the large polymerase complex (Figure 5C). Therefore, a local modification of the conformation of the helical nucleocapsid must take place. Nucleocapsids are flexible and can adopt different conformations [21,109–111]. Such uncoiling and bending could enable the polymerase complex to reach the RNA cavity. Although N_{tail} affects the rigidity and the pitch of the helical nucleocapsids [21,113,117,121], the addition of monomeric P_{XD} to intact nucleocapsids of HeV or MuV does not affect the coiling of the helix [75,114]. For HeV, the addition of P_{XD} does not make the RNA more accessible to nucleases either. Similarly, the binding of the C-terminal domain of VSIV P to NCLC does not significantly modify the structure of the N proteins [210]. This suggests that either the binding of P_{XD} does not participate in the uncoiling of the nucleocapsid, or the oligomerization of P_{XD} is required. Some cellular factors may also contribute to the uncoiling of the nucleocapsid, such as hsp70, which binds MeV N_{tail} [154,163], stimulates MeV and CDV polymerase activity [154,211], and seems to favor the production of "light" nucleocapsids (versus "dense" nucleocapsids) of CDV [212,213]. Conversely, the P_{NTD} of MuV can uncoil the helical nucleocapsid and increase gene expression in a minigenome assay [68,114]. Similar to the binding of MuV P_{XD} to N_{core}, the atypical behavior of MuV P_{NTD} could reflect a possibly common uncoiling mechanism.

Second, the RNA cavity of the N proteins must open to release the RNA upon the passage of the polymerase. A first model proposes that the N protomers undergo a large conformational rearrangement reverting from the N^{NUC} to the N^0 conformation [24,214]. Molecular dynamics simulations show that in absence of ligands (RNA or P_{NTD}), the N protein of PIV5, initially in the N^{NUC} conformation, adopts a conformation similar to the N^0 conformation. This suggests that the N^0 conformation is the most stable in the absence of RNA and adjacent N proteins [26]. However, the removal of the RNA from nucleocapsid-like structures of MuV or VSIV does not significantly change the relative orientation of N_{NTD} and N_{CTD} [179,215]. Moreover, when the simulations are made on a short RNA-free nucleocapsid of three N proteins of PIV5, only the conformations of the N_{i+1} and N_i protomers slightly change toward the N^0 conformation, with the conformation of the N_i protomer being modified to a lower extent. Thus, the conformational rearrangement from

the N^{NUC} to the N^0 conformation may partially take place only at the 3′ end of the genome to facilitate the release of the RNA terminus and the engagement of the polymerase.

Another model proposes that a local conformational change of the α-helix 7 and the upstream flexible loop is enough to release the RNA [215] (Figure 8E). Indeed, this helix, which is located at the surface of the protein, constitutes most of the bottom part of the RNA cavity and contains several amino acids implicated in RNA stabilization. Moreover, when the N_{NTD} of MeV N^{NUC} and N^0 are superimposed, the loop-α7 region is the only fragment that does not properly align (Figure 8E). Thus, in addition to the rotation of the N_{NTD}, the transition from the N^0 to the N^{NUC} conformation also implies a local rearrangement of this region. Mutations in this helix affect gene expression, which is in agreement with a potential role in releasing the RNA during RNA synthesis [215].

P_{NTD} has also been proposed to participate in the release of the RNA. Due to the tight N-N interactions and the high stability of the nucleocapsid, it seems unlikely that during the progression of the polymerase P_{NTD} would bind the N protomers in an N^0-P-like manner and sequentially "open" the N proteins. However, the N_{NTDarm}-binding groove of the last N protomer of the nucleocapsid (or the first protomer on the 3′ terminus) is not occupied and may therefore be engaged by P_{NTD} to help to release the RNA. Due to the binding register of the first six nucleotides of the genome and the rule of six, the terminal 3′ nucleotides are positioned such that they are exposed to the solvent and are therefore more accessible [20]. Therefore, the binding of P_{NTD} only to the terminal N protomer may be sufficient for the polymerase to access the RNA. However, for SeV and hPIV3, the deletion of the P_{NTD} abolishes genome replication but not transcription in vitro, thus suggesting that the potential role of P_{NTD} in releasing the RNA is not essential (at least for members of the *Respirovirus* genus) [216,217].

6. Model of Transcription and Replication

6.1. Transcription

Upon fusion of viral and cellular membranes and the subsequent release of the nucleocapsid in the cytoplasm, the polymerase complexes previously packaged in the virion initiate primary transcription. Given that the nucleocapsid adopts a helical conformation, the two elements of the bipartite promoter are exposed on the same side. P_{XD} binds N_{tail} and recruits the polymerase complex on the nucleocapsid (Figure 11A). When the polymerase reaches the 3′ end of the nucleocapsid, it is somehow stabilized by the second element of the bi-partite promoter (PE2). The phase register of the encapsidation exposes the 3′ end of the genome to the solvent. The release of the RNA from the first N protein may be enhanced by the lodging of one P_{NTD} into the empty N_{NTDarm}-binding groove of the first protomer (Figure 11B). A conformational change of the first two N protomers from the N^{NUC} to the N^0 conformation may also assist the release. When the polymerase complex passes on an N protomer, a transient local conformational change of the helix α7 of N_{NTD} and the preceding loop allows the release of the RNA (Figure 11C).

The progression of the polymerase along the genome induces a local conformational change of the helical nucleocapsid (Figure 11D). A dynamic dance is orchestrated by P_{XD}, which periodically binds the α-MoRE of N_{tail} and N_{core}. The fuzziness of N_{tail} inhibits the passage of the polymerase complex, which uses P_{XD} to "clear the way". First, P_{XD} binds $N_{\alpha\text{-MoRE}}$ which folds upon binding into an alpha-helix (Figure 11E). Second, the $P_{XD}/N_{\alpha\text{-MoRE}}$ complex binds the N_{core} of the same protomer or an adjacent protomer (model 1), thus stabilizing the N_{tail}, decreasing the fuzziness, and facilitating the progression of the polymerase (Figure 11F,G). As the binding of the $P_{XD}/N_{\alpha\text{-MoRE}}$ complex to the N_{NTD} of N protomer from the same helical turn would potentially further block the way (Figure 11F), the complex could alternatively bind the N_{NTD} of a protomer from the previous helical turn (model 2). In this alternative model, the anchoring of the N_{tail} to the previous helical turn would further remove it from the path of the polymerase (Figure 11H–K).

This dynamic interaction network regulates the speed of the RNA synthesis and ensures an optimal recognition of the transcription signals at the intergenic regions (IR) (Figure 2A). Indeed, upon the recognition of the first IR, the polymerase stops the synthesis of the leader RNA and scans the genome to find the next gene start signal (GS). Recognition of the GS triggers the re-initiation of RNA synthesis and capping of the mRNA. If recognized, the gene end signal triggers the synthesis of the poly(A) tail (for more details on the mechanisms of RNA synthesis, see [218]). The efficiency with which the polymerase crosses the IR and scans the genome depends on P_{XD} and its interactions with the nucleocapsid. It is yet to be deciphered if the P_{XD} that binds the L protein can simultaneously bind N_{tail} and if it periodically associates with and dissociates from L.

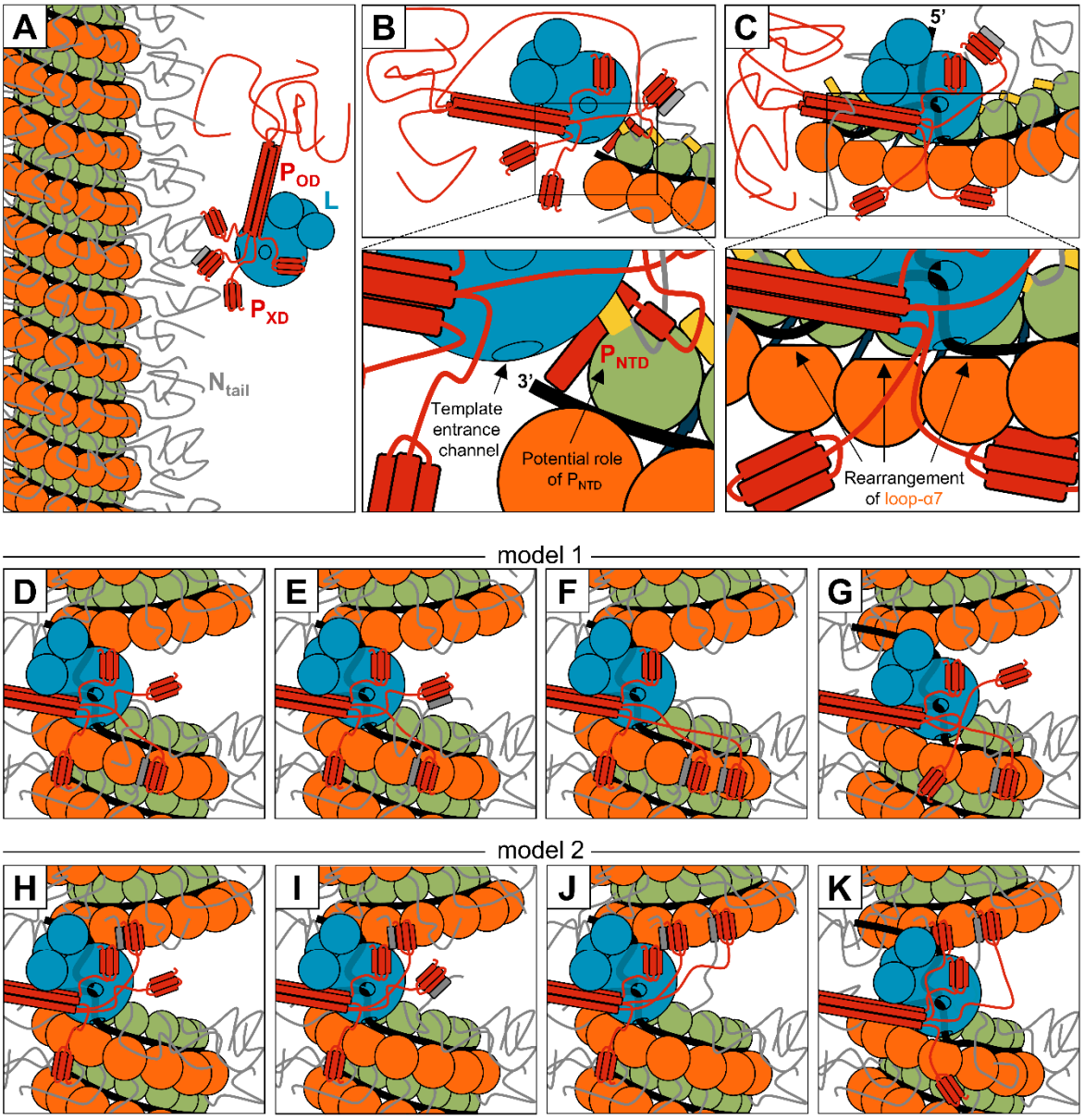

Figure 11. *Cont.*

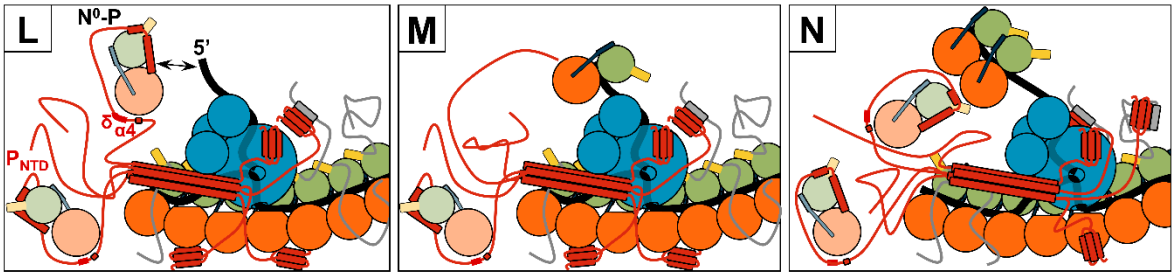

Figure 11. Models of different steps of RNA synthesis. Schematic representations of the recruitment of the polymerase complex (**A**), the initiation of RNA synthesis (**B**), the release of the RNA (**C**), the dynamics of the interaction between P_{XD} and N_{tail} and of P_{XD}-$N_{\alpha\text{-MoRE}}$ with N_{core} (**D**–**K**), and the encapsidation of nascent RNA during replication (**L**–**N**). (**A**) The polymerase complex is recruited on its template via the interaction between P_{XD} and N_{tail}. (**B**) The polymerase complex finds the 3′ end of the genome to initiate RNA synthesis. Bottom panel: enlargement of the top panel. The binding of P_{NTD} to the first protomer may enhance the release of the RNA and its engagement in the template entrance channel. (**C**) The progression of the polymerase complex induces a local rearrangement of the helix α7 and the preceding loop. This conformational change releases the RNA. (**D**–**K**) Two models are proposed for the dynamics of the interaction between P_{XD} and N during the progression of the polymerase complex. (**D**,**H**) In both cases, the polymerase induces a local conformational change on the helical nucleocapsid. The N_{tail} are flexible, disordered, and inhibit the progression of the polymerase complex. (**E**,**I**) P_{XD} binds N_{tail} and induces the folding of the $N_{\alpha\text{-MoRE}}$. (**F**) In model 1, the $P_{XD}/N_{\alpha\text{-MoRE}}$ complex binds the N_{core} of the next N protomer. (**G**) The stabilization of N_{tail} by P_{XD} allows the polymerase complex to continue RNA synthesis. (**J**) In model 2, the $P_{XD}/N_{\alpha\text{-MoRE}}$ complex binds the N_{core} of an N protomer from the previous helical turn. (**K**) The anchoring of the N_{tail} to the previous helical turn "clears the way" and allows an efficient progression of the polymerase complex. (**L**) During replication, some P_{NTD} are bound to N^0 monomers. The N^0-P complex is stabilized by the transient α4 and the preceding delta domain. N^0 has a strong affinity for the first six residues of the viral genome. (**M**) N^0 is transferred onto the nascent RNA and switches from the N^0 to the N^{NUC} conformation. (**N**) Thanks to interactions between the N^0 and the last N protomer added on the nascent RNA, the N proteins can be added to the growing polymerase even if the affinity for the RNA sequence is low. For N, the color code is the same as in Figure 4.

6.2. Replication

After new viral proteins have been synthesized, the polymerase complex switches from a transcriptase mode to a replicase mode. The details of this switch are not fully understood, but the accumulation of the encapsidation substrate, the N^0-P complex, plays a key role in this process. In the replicase mode, the polymerase complex encapsidates the nascent RNA and does not recognize any transcription signals. As the N protein has a higher affinity for an RNA with the sequence of the 5′ end of the genome, the first six nucleotides of the nascent genome outcompete P_{NTD} for the binding to N (Figure 11L,M). For the following N protomers, P_{NTD} is outcompeted by both the RNA and the N_{CTDarm} of the previous N protomer (Figure 11N). This double competition allows the continuous encapsidation of any RNA sequences, even with a poor affinity for N, such as poly(U) sequences.

7. Conclusions and Perspectives

In recent years, several significant advances have been made which add to our understanding of the structure and mechanisms of the molecular machinery underlying RNA synthesis of paramyxoviruses. We now have in hand structural information on the N^0-P complex and the nucleocapsid of three and seven viruses, respectively. The determination of the phase register of the encapsidated RNA further reveals the mechanisms underlying the rule of six. Moreover, the deciphering of the rich interaction network connecting the different components of the ribonucleoprotein complex gives us a good overview of the dynamics of the progression of the polymerase complex. Finally, the resolution of the atomic structure of the polymerase complex of PIV5 provides a new tool and opens new opportunities to further elucidate the molecular details of the RNA synthesis.

Except for MuV and its atypical features (antiparallel coiled-coil for P_{OD}, unstable P_{XD} in solution, interaction between P_{XD} and N_{core} in the absence of N_{tail}, and uncoiling of

the nucleocapsid by P_{NTD}), the molecular machinery and the mechanisms at play during RNA synthesis appear to be well conserved among paramyxoviruses. The exposure of the RNA on the outside of the helical nucleocapsid, the binding site of the C-terminal domain of P to the N_{NTD}, the coiled-coil structure of P_{OD}, and the interaction sites between P and L suggest these mechanisms are shared with pneumoviruses and filoviruses but are quite different for rhabdoviruses.

Despite these new insights, several questions remain unanswered. The helical nucleocapsid must uncoil to allow the progression of the polymerase. What factors induce this conformational change? It is also still unclear how the nucleoproteins release the RNA and what signals trigger this release. Although structural information is available on the individual components, there is little insight into the organization or the structure of the polymerase complex on the nucleocapsid while synthesizing RNA. In addition, how does the second element of the bipartite promoter enhance initiation? How does the polymerase complex add nucleoproteins to the nascent RNA? How does the phosphoprotein orchestrate its interactions with N_{tail}, N_{core}, and L? How do other viral proteins such as the V, C, and M proteins interact with the ribonucleoprotein complex and regulate RNA synthesis?

Answering these questions should bring significant insight into the mechanisms at play and assist the development of safe and potent vaccine vectors, oncolytic viruses, and antiviral therapeutics. With the momentum provided by the recent advances and the constant improvement of powerful tools such as cryo-electron microscopy, there is no doubt our understanding of the viral molecular machinery of paramyxoviruses will continue to rapidly improve.

Funding: This work was supported by NIH grant AI059371 to Sean P.J. Whelan.

Acknowledgments: I thank Denis Gerlier and Sonia Longhi for their helpful comments and suggestions, Paul W. Rothlauf for the English proofreading of the manuscript, Sean P.J. Whelan for his support, and Soazig Friguel for her help in assembling the figures.

Conflicts of Interest: The author declares no conflict of interest.

References

1. Rima, B.; Balkema-Buschmann, A.; Dundon, W.G.; Duprex, P.; Easton, A.; Fouchier, R.; Kurath, G.; Lamb, R.; Lee, B.; Rota, P.; et al. ICTV Virus Taxonomy Profile: Paramyxoviridae. *J. Gen. Virol.* **2019**, *100*, 1593–1594. [CrossRef] [PubMed]
2. Cox, R.; Plemper, R.K. The paramyxovirus polymerase complex as a target for next-generation anti-paramyxovirus therapeutics. *Front. Microbiol.* **2015**, *6*, 459. [CrossRef] [PubMed]
3. Aggarwal, M.; Plemper, R.K. Structural Insight into Paramyxovirus and Pneumovirus Entry Inhibition. *Viruses* **2020**, *12*, 342. [CrossRef] [PubMed]
4. Emerson, S.U.; Wagner, R.R. Dissociation and reconstitution of the transcriptase and template activities of vesicular stomatitis B and T virions. *J. Virol.* **1972**, *10*, 297–309. [CrossRef] [PubMed]
5. Emerson, S.U.; Yu, Y. Both NS and L proteins are required for in vitro RNA synthesis by vesicular stomatitis virus. *J. Virol.* **1975**, *15*, 1348–1356. [CrossRef]
6. Hamaguchi, M.; Yoshida, T.; Nishikawa, K.; Naruse, H.; Nagai, Y. Transcriptive complex of Newcastle disease virus. I. Both L and P proteins are required to constitute an active complex. *Virology* **1983**, *128*, 105–117. [CrossRef]
7. Horikami, S.M.; Curran, J.; Kolakofsky, D.; Moyer, S.A. Complexes of Sendai virus NP-P and P-L proteins are required for defective interfering particle genome replication in vitro. *J. Virol.* **1992**, *66*, 4901–4908. [CrossRef]
8. Stone, H.O.; Kingsbury, D.W.; Darlington, R.W. Sendai virus-induced transcriptase from infected cells: Polypeptides in the transcriptive complex. *J. Virol.* **1972**, *10*, 1037–1043. [CrossRef]
9. Colonno, R.J.; Stone, H.O. Isolation of a transcriptive complex from Newcastle disease virions. *J. Virol.* **1976**, *19*, 1080–1089. [CrossRef]
10. Portner, A.; Murti, K.G.; Morgan, E.M.; Kingsbury, D.W. Antibodies against Sendai virus L protein: Distribution of the protein in nucleocapsids revealed by immunoelectron microscopy. *Virology* **1988**, *163*, 236–239. [CrossRef]
11. Mura, M.; Combredet, C.; Najburg, V.; David, R.Y.S.; Tangy, F.; Komarova, A.V. Nonencapsidated 5′ Copy-Back Defective Interfering Genomes Produced by Recombinant Measles Viruses Are Recognized by RIG-I and LGP2 but Not MDA5. *J. Virol.* **2017**, *91*. [CrossRef] [PubMed]
12. Nilsson-Payant, B.E.; Blanco-Melo, D.; Uhl, S.; Escudero-Pérez, B.; Olschewski, S.; Thibault, P.; Panis, M.; Rosenthal, M.; Muñoz-Fontela, C.; Lee, B.; et al. Reduced Nucleoprotein Availability Impairs Negative-Sense RNA Virus Replication and Promotes Host Recognition. *J. Virol.* **2021**, *95*, e02274-20. [CrossRef] [PubMed]

13. Compans, R.W.; Choppin, P.W. The nucleic acid of the parainfluenza virus SV5. *Virology* **1968**, *35*, 289–296. [CrossRef]
14. Lynch, S.; Kolakofsky, D. Ends of the RNA within Sendai virus defective interfering nucleocapsids are not free. *J. Virol.* **1978**, *28*, 584–589. [CrossRef]
15. Bitko, V.; Barik, S. Phenotypic silencing of cytoplasmic genes using sequence-specific double-stranded short interfering RNA and its application in the reverse genetics of wild type negative-strand RNA viruses. *BMC Microbiol.* **2001**, *1*, 34. [CrossRef] [PubMed]
16. Mottet-Osman, G.; Iseni, F.; Pelet, T.; Wiznerowicz, M.; Garcin, D.; Roux, L. Suppression of the Sendai Virus M Protein through a Novel Short Interfering RNA Approach Inhibits Viral Particle Production but Does Not Affect Viral RNA Synthesis. *J. Virol.* **2007**, *81*, 2861–2868. [CrossRef]
17. Alayyoubi, M.; Leser, G.P.; Kors, C.A.; Lamb, R.A. Structure of the paramyxovirus parainfluenza virus 5 nucleoprotein-RNA complex. *Proc. Natl. Acad. Sci. USA* **2015**, *112*, E1792–E1799. [CrossRef]
18. Gutsche, I.; Desfosses, A.; Effantin, G.; Ling, W.L.; Haupt, M.; Ruigrok, R.W.H.; Sachse, C.; Schoehn, G. Near-atomic cryo-EM structure of the helical measles virus nucleocapsid. *Science* **2015**, *348*, 704–707. [CrossRef]
19. Song, X.; Shan, H.; Zhu, Y.; Hu, S.; Xue, L.; Chen, Y.; Ding, W.; Niu, T.; Gu, J.; Ouyang, S.; et al. Self-capping of nucleoprotein filaments protects the Newcastle disease virus genome. *eLife* **2019**, *8*. [CrossRef]
20. Desfosses, A.; Milles, S.; Jensen, M.R.; Guseva, S.; Colletier, J.-P.; Maurin, D.; Schoehn, G.; Gutsche, I.; Ruigrok, R.W.H.; Blackledge, M. Assembly and cryo-EM structures of RNA-specific measles virus nucleocapsids provide mechanistic insight into paramyxoviral replication. *Proc. Natl. Acad. Sci. USA* **2019**, *116*, 4256–4264. [CrossRef] [PubMed]
21. Zhang, N.; Shan, H.; Liu, M.; Li, T.; Luo, R.; Yang, L.; Qi, L.; Chu, X.; Su, X.; Wang, R.; et al. Structure and assembly of double-headed Sendai virus nucleocapsids. *Commun. Biol.* **2021**, *4*, 494. [CrossRef]
22. Ker, D.-S.; Jenkins, H.T.; Greive, S.J.; Antson, A.A. CryoEM structure of the Nipah virus nucleocapsid assembly. *PLoS Pathog.* **2021**, *17*, e1009740. [CrossRef]
23. Zinzula, L.; Beck, F.; Klumpe, S.; Bohn, S.; Pfeifer, G.; Bollschweiler, D.; Nagy, I.; Plitzko, J.M.; Baumeister, W. Cryo-EM structure of the cetacean morbillivirus nucleoprotein-RNA complex. *J. Struct. Biol.* **2021**, *213*, 107750. [CrossRef] [PubMed]
24. Yabukarski, F.; Lawrence, P.; Tarbouriech, N.; Bourhis, J.-M.; Delaforge, E.; Jensen, M.R.; Ruigrok, R.W.H.; Blackledge, M.; Volchkov, V.; Jamin, M. Structure of Nipah virus unassembled nucleoprotein in complex with its viral chaperone. *Nat. Struct. Mol. Biol.* **2014**, *21*, 754–759. [CrossRef]
25. Guryanov, S.G.; Liljeroos, L.; Kasaragod, P.; Kajander, T.; Butcher, S.J. Crystal Structure of the Measles Virus Nucleoprotein Core in Complex with an N-Terminal Region of Phosphoprotein. *J. Virol.* **2016**, *90*, 2849–2857. [CrossRef]
26. Aggarwal, M.; Leser, G.P.; Kors, C.A.; Lamb, R.A. Structure of the Paramyxovirus Parainfluenza Virus 5 Nucleoprotein in Complex with an Amino-Terminal Peptide of the Phosphoprotein. *J. Virol.* **2018**, *92*, e01304-17. [CrossRef] [PubMed]
27. Dong, X.; Wang, X.; Xie, M.; Wu, W.; Chen, Z. Structural Basis of Human Parainfluenza Virus 3 Unassembled Nucleoprotein in Complex with Its Viral ChaperoneHPIV3 Nucleoprotein-Phosphoprotein Structure. *J. Virol.* **2021**, JVI0164821. [CrossRef]
28. Abdella, R.; Aggarwal, M.; Okura, T.; Lamb, R.A.; He, Y. Structure of a paramyxovirus polymerase complex reveals a unique methyltransferase-CTD conformation. *Proc. Natl. Acad. Sci. USA* **2020**, *117*, 4931–4941. [CrossRef]
29. Glazier, K.; Raghow, R.; Kingsbury, D.W. Regulation of Sendai virus transcription: Evidence for a single promoter in vivo. *J. Virol.* **1977**, *21*, 863–871. [CrossRef]
30. Le Mercier, P.; Kolakofsky, D. Bipartite promoters and RNA editing of paramyxoviruses and filoviruses. *RNA* **2019**, *25*, 279–285. [CrossRef] [PubMed]
31. Plemper, R.K.; Lamb, R.A. Paramyxoviridae: The viruses and their replication. In *Fields Virology: Emerging Viruses*, 7th ed.; Howley, P.M., Knipe, D.M., Eds.; Lippincott Williams and Wilkins, Wolters Kluwer: Philadelphia, PA, USA, 2020; pp. 504–558.
32. Calain, P.; Roux, L. The rule of six, a basic feature for efficient replication of Sendai virus defective interfering RNA. *J. Virol.* **1993**, *67*, 4822–4830. [CrossRef] [PubMed]
33. Kolakofsky, D.; Pelet, T.; Garcin, D.; Hausmann, S.; Curran, J.; Roux, L. Paramyxovirus RNA synthesis and the requirement for hexamer genome length: The rule of six revisited. *J. Virol.* **1998**, *72*, 891–899. [CrossRef]
34. Longhi, S.; Receveur-Brechot, V.; Karlin, D.; Johansson, K.; Darbon, H.; Bhella, D.; Yeo, R.; Finet, S.; Canard, B. The C-terminal Domain of the Measles Virus Nucleoprotein Is Intrinsically Disordered and Folds upon Binding to the C-terminal Moiety of the Phosphoprotein. *J. Biol. Chem.* **2003**, *278*, 18638–18648. [CrossRef] [PubMed]
35. Mountcastle, W.E.; Compans, R.W.; Lackland, H.; Choppin, P.W. Proteolytic cleavage of subunits of the nucleocapsid of the paramyxovirus simian virus 5. *J. Virol.* **1974**, *14*, 1253–1261. [CrossRef] [PubMed]
36. Buchholz, C.J.; Spehner, D.; Drillien, R.; Neubert, W.J.; Homann, H.E. The conserved N-terminal region of Sendai virus nucleocapsid protein NP is required for nucleocapsid assembly. *J. Virol.* **1993**, *67*, 5803–5812. [CrossRef]
37. Curran, J.; Homann, H.; Buchholz, C.; Rochat, S.; Neubert, W.; Kolakofsky, D. The hypervariable C-terminal tail of the Sendai paramyxovirus nucleocapsid protein is required for template function but not for RNA encapsidation. *J. Virol.* **1993**, *67*, 4358–4364. [CrossRef] [PubMed]
38. Bankamp, B.; Horikami, S.M.; Thompson, P.; Huber, M.; Billeter, M.; Moyer, S.A. Domains of the Measles Virus N Protein Required for Binding to P Protein and Self-Assembly. *Virology* **1996**, *216*, 272–277. [CrossRef] [PubMed]
39. Buchholz, C.J.; Retzler, C.; Homann, H.E.; Neubert, W.J. The Carboxy-terminal Domain of Sendai Virus Nucleocapsid Protein Is Involved in Complex Formation between Phosphoprotein and Nucleocapsid-like Particles. *Virology* **1994**, *204*, 770–776. [CrossRef] [PubMed]

40. Liston, P.; Batal, R.; Diflumeri, C.; Briedis, D.J. Protein interaction domains of the measles virus nucleocapsid protein (NP). *Arch. Virol.* **1997**, *142*, 305–321. [CrossRef]
41. Rahmeh, A.A.; Schenk, A.; Danek, E.I.; Kranzusch, P.J.; Liang, B.; Walz, T.; Whelan, S.P.J. Molecular architecture of the vesicular stomatitis virus RNA polymerase. *Proc. Natl. Acad. Sci. USA* **2010**, *107*, 20075–20080. [CrossRef]
42. Liang, B. Structures of the *Mononegavirales* Polymerases. *J. Virol.* **2020**, *94*, e00175-20. [CrossRef]
43. Pyle, J.D.; Whelan, S.P.; Bloyet, L.-M. Structure and function of negative-strand RNA virus polymerase complexes. *Enzymes* **2021**, *50*, 21–78. [CrossRef]
44. Abraham, G.; Rhodes, D.P.; Banerjee, A.K. Novel initiation of RNA synthesis in vitro by vesicular stomatitis virus. *Nature* **1975**, *255*, 37–40. [CrossRef] [PubMed]
45. Ogino, T.; Banerjee, A.K. Unconventional Mechanism of mRNA Capping by the RNA-Dependent RNA Polymerase of Vesicular Stomatitis Virus. *Mol. Cell* **2007**, *25*, 85–97. [CrossRef]
46. Hercyk, N.; Horikami, S.M.; Moyer, S.A. The vesicular stomatitis virus L protein possesses the mRNA methyltransferase activities. *Virology* **1988**, *163*, 222–225. [CrossRef]
47. Ogino, T.; Kobayashi, M.; Iwama, M.; Mizumoto, K. Sendai Virus RNA-dependent RNA Polymerase L Protein Catalyzes Cap Methylation of Virus-specific mRNA. *J. Biol. Chem.* **2005**, *280*, 4429–4435. [CrossRef]
48. Hunt, D.M.; Mehta, R.; Hutchinson, K.L. The L Protein of Vesicular Stomatitis Virus Modulates the Response of the Polyadenylic Acid Polymerase to S-Adenosylhomocysteine. *J. Gen. Virol.* **1988**, *69*, 2555–2561. [CrossRef]
49. Jordan, P.C.; Liu, C.; Raynaud, P.; Lo, M.; Spiropoulou, C.F.; Symons, J.A.; Beigelman, L.; Deval, J. Initiation, extension, and termination of RNA synthesis by a paramyxovirus polymerase. *PLoS Pathog.* **2018**, *14*, e1006889. [CrossRef] [PubMed]
50. Smallwood, S.; Ryan, K.W.; Moyer, S.A. Deletion Analysis Defines a Carboxyl-Proximal Region of Sendai Virus P Protein That Binds to the Polymerase L Protein. *Virology* **1994**, *202*, 154–163. [CrossRef] [PubMed]
51. Canter, D.; Perrault, J. Stabilization of Vesicular Stomatitis Virus L Polymerase Protein by P Protein Binding: A Small Deletion in the C-Terminal Domain of L Abrogates Binding. *Virology* **1996**, *219*, 376–386. [CrossRef] [PubMed]
52. Bloyet, L.-M.; Welsch, J.; Enchery, F.; Mathieu, C.; de Breyne, S.; Horvat, B.; Grigorov, B.; Gerlier, D. HSP90 Chaperoning in Addition to Phosphoprotein Required for Folding but Not for Supporting Enzymatic Activities of Measles and Nipah Virus L Polymerases. *J. Virol.* **2016**, *90*, 6642–6656. [CrossRef]
53. Mellon, M.G.; Emerson, S.U. Rebinding of transcriptase components (L and NS proteins) to the nucleocapsid template of vesicular stomatitis virus. *J. Virol.* **1978**, *27*, 560–567. [CrossRef] [PubMed]
54. Masters, P.S.; Banerjee, A.K. Complex formation with vesicular stomatitis virus phosphoprotein NS prevents binding of nucleocapsid protein N to nonspecific RNA. *J. Virol.* **1988**, *62*, 2658–2664. [CrossRef] [PubMed]
55. Curran, J.; Marq, J.B.; Kolakofsky, D. An N-terminal domain of the Sendai paramyxovirus P protein acts as a chaperone for the NP protein during the nascent chain assembly step of genome replication. *J. Virol.* **1995**, *69*, 849–855. [CrossRef]
56. Spehner, D.; Drillien, R.; Howley, P.M. The Assembly of the Measles Virus Nucleoprotein into Nucleocapsid-like Particles Is Modulated by the Phosphoprotein. *Virology* **1997**, *232*, 260–268. [CrossRef] [PubMed]
57. Karlin, D.; Ferron, F.; Canard, B.; Longhi, S. Structural disorder and modular organization in Paramyxovirinae N and P. *J. Gen. Virol.* **2003**, *84*, 3239–3252. [CrossRef]
58. Gerard, F.C.; Ribeiro, E.D.A.; Leyrat, C.; Ivanov, I.; Blondel, D.; Longhi, S.; Ruigrok, R.W.; Jamin, M. Modular Organization of Rabies Virus Phosphoprotein. *J. Mol. Biol.* **2009**, *388*, 978–996. [CrossRef] [PubMed]
59. Habchi, J.; Mamelli, L.; Darbon, H.; Longhi, S. Structural Disorder within Henipavirus Nucleoprotein and Phosphoprotein: From Predictions to Experimental Assessment. *PLoS ONE* **2010**, *5*, e11684. [CrossRef]
60. Pereira, N.; Cardone, C.; Lassoued, S.; Galloux, M.; Fix, J.; Assrir, N.; Lescop, E.; Bontems, F.; Eléouët, J.-F.; Sizun, C. New Insights into Structural Disorder in Human Respiratory Syncytial Virus Phosphoprotein and Implications for Binding of Protein Partners. *J. Biol. Chem.* **2017**, *292*, 2120–2131. [CrossRef] [PubMed]
61. Longhi, S.; Bloyet, L.-M.; Gianni, S.; Gerlier, D. How order and disorder within paramyxoviral nucleoproteins and phosphoproteins orchestrate the molecular interplay of transcription and replication. *Cell. Mol. Life Sci.* **2017**, *74*, 3091–3118. [CrossRef]
62. Jensen, M.R.; Yabukarski, F.; Communie, G.; Condamine, E.; Mas, C.; Volchkova, V.; Tarbouriech, N.; Bourhis, J.-M.; Volchkov, V.; Blackledge, M.; et al. Structural Description of the Nipah Virus Phosphoprotein and Its Interaction with STAT1. *Biophys. J.* **2020**, *118*, 2470–2488. [CrossRef]
63. Tarbouriech, N.; Curran, J.; Ruigrok, R.W.; Burmeister, W.P. Tetrameric coiled coil domain of Sendai virus phosphoprotein. *Nat. Genet.* **2000**, *7*, 777–781. [CrossRef]
64. Communie, G.; Crepin, T.; Maurin, D.; Jensen, M.R.; Blackledge, M.; Ruigrok, R.W.H. Structure of the Tetramerization Domain of Measles Virus Phosphoprotein. *J. Virol.* **2013**, *87*, 7166–7169. [CrossRef] [PubMed]
65. Blocquel, D.; Habchi, J.; Durand, E.; Sevajol, M.; Ferron, F.; Erales, J.; Papageorgiou, N.; Longhi, S. Coiled-coil deformations in crystal structures: The measles virus phosphoprotein multimerization domain as an illustrative example. *Acta Crystallogr. D Biol. Crystallogr.* **2014**, *70*, 1589–1603. [CrossRef] [PubMed]
66. Bruhn, J.F.; Barnett, K.; Bibby, J.; Thomas, J.M.H.; Keegan, R.; Rigden, D.J.; Bornholdt, Z.A.; Saphire, E.O. Crystal Structure of the Nipah Virus Phosphoprotein Tetramerization Domain. *J. Virol.* **2013**, *88*, 758–762. [CrossRef]

67. Galvan, J.R.; Donner, B.; Veseley, C.H.; Reardon, P.; Forsythe, H.M.; Howe, J.; Fujimura, G.; Barbar, E. Human Parainfluenza Virus 3 Phosphoprotein Is a Tetramer and Shares Structural and Interaction Features with Ebola Phosphoprotein VP35. *Biomolecules* **2021**, *11*, 1603. [CrossRef] [PubMed]
68. Cox, R.; Green, T.J.; Purushotham, S.; Deivanayagam, C.; Bedwell, G.J.; Prevelige, P.E.; Luo, M. Structural and Functional Characterization of the Mumps Virus Phosphoprotein. *J. Virol.* **2013**, *87*, 7558–7568. [CrossRef] [PubMed]
69. Pickar, A.; Elson, A.; Yang, Y.; Xu, P.; Luo, M.; He, B. Oligomerization of Mumps Virus Phosphoprotein. *J. Virol.* **2015**, *89*, 11002–11010. [CrossRef]
70. Ryan, K.W.; Kingsbury, D.W. Carboxyl-terminal region of sendai virus P protein is required for binding to viral nucleocapsids. *Virology* **1988**, *167*, 106–112. [CrossRef]
71. Johansson, K.; Bourhis, J.-M.; Campanacci, V.; Cambillau, C.; Canard, B.; Longhi, S. Crystal Structure of the Measles Virus Phosphoprotein Domain Responsible for the Induced Folding of the C-terminal Domain of the Nucleoprotein. *J. Biol. Chem.* **2003**, *278*, 44567–44573. [CrossRef] [PubMed]
72. Blanchard, L.; Tarbouriech, N.; Blackledge, M.; Timmins, P.; Burmeister, W.P.; Ruigrok, R.W.; Marion, D. Structure and dynamics of the nucleocapsid-binding domain of the Sendai virus phosphoprotein in solution. *Virology* **2004**, *319*, 201–211. [CrossRef]
73. Kingston, R.L.; Hamel, D.J.; Gay, L.S.; Dahlquist, F.W.; Matthews, B.W. Structural basis for the attachment of a paramyxoviral polymerase to its template. *Proc. Natl. Acad. Sci. USA* **2004**, *101*, 8301–8306. [CrossRef]
74. Habchi, J.; Blangy, S.; Mamelli, L.; Jensen, M.R.; Blackledge, M.; Darbon, H.; Oglesbee, M.; Shu, Y.; Longhi, S. Characterization of the Interactions between the Nucleoprotein and the Phosphoprotein of Henipavirus. *J. Biol. Chem.* **2011**, *286*, 13583–13602. [CrossRef] [PubMed]
75. Communie, G.; Habchi, J.; Yabukarski, F.; Blocquel, D.; Schneider, R.; Tarbouriech, N.; Papageorgiou, N.; Ruigrok, R.W.H.; Jamin, M.; Jensen, M.R.; et al. Atomic Resolution Description of the Interaction between the Nucleoprotein and Phosphoprotein of Hendra Virus. *PLoS Pathog.* **2013**, *9*, e1003631. [CrossRef] [PubMed]
76. Blumberg, B.M.; Leppert, M.; Kolakofsky, D. Interaction of VSV leader RNA and nucleocapsid protein may control VSV genome replication. *Cell* **1981**, *23*, 837–845. [CrossRef]
77. Plumet, S.; Duprex, W.P.; Gerlier, D. Dynamics of Viral RNA Synthesis during Measles Virus Infection. *J. Virol.* **2005**, *79*, 6900–6908. [CrossRef]
78. Ranadheera, C.; Proulx, R.; Chaiyakul, M.; Jones, S.; Grolla, A.; Leung, A.; Rutherford, J.; Kobasa, D.; Carpenter, M.; Czub, M. The interaction between the Nipah virus nucleocapsid protein and phosphoprotein regulates virus replication. *Sci. Rep.* **2018**, *8*, 15994. [CrossRef] [PubMed]
79. Gubbay, O.; Curran, J.; Kolakofsky, D. Sendai virus genome synthesis and assembly are coupled: A possible mechanism to promote viral RNA polymerase processivity. *J. Gen. Virol.* **2001**, *82*, 2895–2903. [CrossRef] [PubMed]
80. Guseva, S.; Milles, S.; Jensen, M.R.; Schoehn, G.; Ruigrok, R.W.; Blackledge, M. Structure, dynamics and phase separation of measles virus RNA replication machinery. *Curr. Opin. Virol.* **2020**, *41*, 59–67. [CrossRef]
81. Nikolic, J.; Lagaudrière-Gesbert, C.; Scrima, N.; Blondel, D.; Gaudin, Y. Structure and Function of Negri Bodies. *Adv. Exp. Med. Biol.* **2019**, *1215*, 111–127. [CrossRef] [PubMed]
82. Brocca, S.; Grandori, R.; Longhi, S.; Uversky, V. Liquid-Liquid Phase Separation by Intrinsically Disordered Protein Regions of Viruses: Roles in Viral Life Cycle and Control of Virus-Host Interactions. *Int. J. Mol. Sci.* **2020**, *21*, 9045. [CrossRef] [PubMed]
83. Hagiwara, K.; Sato, H.; Inoue, Y.; Watanabe, A.; Yoneda, M.; Ikeda, F.; Fujita, K.; Fukuda, H.; Takamura, C.; Kozuka-Hata, H.; et al. Phosphorylation of measles virus nucleoprotein upregulates the transcriptional activity of minigenomic RNA. *Proteomics* **2008**, *8*, 1871–1879. [CrossRef] [PubMed]
84. Huang, M.; Sato, H.; Hagiwara, K.; Watanabe, A.; Sugai, A.; Ikeda, F.; Kozuka-Hata, H.; Oyama, M.; Yoneda, M.; Kai, C. Determination of a phosphorylation site in Nipah virus nucleoprotein and its involvement in virus transcription. *J. Gen. Virol.* **2011**, *92*, 2133–2141. [CrossRef] [PubMed]
85. Zengel, J.; Pickar, A.; Xu, P.; Lin, A.; He, B. Roles of Phosphorylation of the Nucleocapsid Protein of Mumps Virus in Regulating Viral RNA Transcription and Replication. *J. Virol.* **2015**, *89*, 7338–7347. [CrossRef]
86. Vidal, S.; Curran, J.; Orvell, C.; Kolakofsky, D. Mapping of monoclonal antibodies to the Sendai virus P protein and the location of its phosphates. *J. Virol.* **1988**, *62*, 2200–2203. [CrossRef]
87. Das, T.; Schuster, A.; Schneider-Schaulies, S.; Banerjee, A.K. Involvement of Cellular Casein Kinase II in the Phosphorylation of Measles Virus P Protein: Identification of Phosphorylation Sites. *Virology* **1995**, *211*, 218–226. [CrossRef] [PubMed]
88. Huntley, C.C.; De, B.P.; Murray, N.R.; Fields, A.P.; Banerjee, A.K. Human parainfluenza virus type 3 phosphoprotein: Identification of serine 333 as the major site for PKC zeta phosphorylation. *Virology* **1995**, *211*, 561–567. [CrossRef]
89. Byrappa, S.; Pan, Y.-B.; Gupta, K.C. Sendai Virus P Protein Is Constitutively Phosphorylated at Serine249: High Phosphorylation Potential of the P Protein. *Virology* **1996**, *216*, 228–234. [CrossRef]
90. Timani, K.A.; Sun, D.; Sun, M.; Keim, C.; Lin, Y.; Schmitt, P.T.; Schmitt, A.; He, B. A Single Amino Acid Residue Change in the P Protein of Parainfluenza Virus 5 Elevates Viral Gene Expression. *J. Virol.* **2008**, *82*, 9123–9133. [CrossRef]
91. Sun, D.; Luthra, P.; Xu, P.; Yoon, H.; He, B. Identification of a Phosphorylation Site within the P Protein Important for mRNA Transcription and Growth of Parainfluenza Virus 5. *J. Virol.* **2011**, *85*, 8376–8385. [CrossRef]
92. Sugai, A.; Sato, H.; Yoneda, M.; Kai, C. Phosphorylation of measles virus phosphoprotein at S86 and/or S151 downregulates viral transcriptional activity. *FEBS Lett.* **2012**, *586*, 3900–3907. [CrossRef] [PubMed]

93. Pickar, A.; Xu, P.; Elson, A.; Li, Z.; Zengel, J.; He, B. Roles of Serine and Threonine Residues of Mumps Virus P Protein in Viral Transcription and Replication. *J. Virol.* **2014**, *88*, 4414–4422. [CrossRef]
94. Qiu, X.; Zhan, Y.; Meng, C.; Wang, J.; Dong, L.; Sun, Y.; Tan, L.; Song, C.; Yu, S.; Ding, C. Identification and functional analysis of phosphorylation in Newcastle disease virus phosphoprotein. *Arch. Virol.* **2016**, *161*, 2103–2116. [CrossRef]
95. De, B.P.; Gupta, S.; Banerjee, A.K. Cellular protein kinase C isoform zeta regulates human parainfluenza virus type 3 replication. *Proc. Natl. Acad. Sci. USA* **1995**, *92*, 5204–5208. [CrossRef]
96. Liu, Z.; Huntley, C.C.; De, B.P.; Das, T.; Banerjee, A.K.; Oglesbee, M.J. Phosphorylation of canine distemper virus P protein by protein kinase C-zeta and casein kinase II. *Virology* **1997**, *232*, 198–206. [CrossRef]
97. Huntley, C.C.; De, B.P.; Banerjee, A.K. Phosphorylation of Sendai virus phosphoprotein by cellular protein kinase C zeta. *J. Biol. Chem.* **1997**, *272*, 16578–16584. [CrossRef]
98. Kaushik, R.; Shaila, M.S. Cellular casein kinase II-mediated phosphorylation of rinderpest virus P protein is a prerequisite for its role in replication/transcription of the genome. *J. Gen. Virol.* **2004**, *85*, 687–691. [CrossRef] [PubMed]
99. Sun, M.; Fuentes, S.M.; Timani, K.; Sun, D.; Murphy, C.; Lin, Y.; August, A.; Teng, M.N.; He, B. Akt Plays a Critical Role in Replication of Nonsegmented Negative-Stranded RNA Viruses. *J. Virol.* **2008**, *82*, 105–114. [CrossRef]
100. Sun, D.; Luthra, P.; Li, Z.; He, B. PLK1 Down-Regulates Parainfluenza Virus 5 Gene Expression. *PLoS Pathog.* **2009**, *5*, e1000525. [CrossRef]
101. Sugai, A.; Sato, H.; Yoneda, M.; Kai, C. PIM 3 kinase, a proto-oncogene product, regulates phosphorylation of the measles virus nucleoprotein tail domain at Ser 479 and Ser 510. *Biochem. Biophys. Res. Commun.* **2020**, *531*. [CrossRef]
102. Young, D.F.; Wignall-Fleming, E.B.; Busse, D.C.; Pickin, M.J.; Hankinson, J.; Randall, E.M.; Tavendale, A.; Davison, A.J.; Lamont, D.; Tregoning, J.S.; et al. The switch between acute and persistent paramyxovirus infection caused by single amino acid substitutions in the RNA polymerase P subunit. *PLoS Pathog.* **2019**, *15*, e1007561. [CrossRef] [PubMed]
103. Saikia, P.; Gopinath, M.; Shaila, M.S. Phosphorylation status of the phosphoprotein P of rinderpest virus modulates transcription and replication of the genome. *Arch. Virol.* **2008**, *153*, 615–626. [CrossRef] [PubMed]
104. Sugai, A.; Sato, H.; Yoneda, M.; Kai, C. Phosphorylation of Measles Virus Nucleoprotein Affects Viral Growth by Changing Gene Expression and Genomic RNA Stability. *J. Virol.* **2013**, *87*, 11684–11692. [CrossRef] [PubMed]
105. Sugai, A.; Sato, H.; Hagiwara, K.; Kozuka-Hata, H.; Oyama, M.; Yoneda, M.; Kai, C. Newly Identified Minor Phosphorylation Site Threonine-279 of Measles Virus Nucleoprotein Is a Prerequisite for Nucleocapsid Formation. *J. Virol.* **2013**, *88*, 1140–1149. [CrossRef]
106. Zhou, Y.; Su, J.M.; Samuel, C.E.; Ma, D. Measles Virus Forms Inclusion Bodies with Properties of Liquid Organelles. *J. Virol.* **2019**, *93*, e00948-19. [CrossRef]
107. Horne, R.W.; Waterson, A.P.; Wildy, P.; Farnham, A.E. The structure and composition of the myxoviruses. I. Electron microscope studies of the structure of myxovirus particles by negative staining techniques. *Virology* **1960**, *11*, 79–98. [CrossRef]
108. Compans, R.; Choppin, P.W. Isolation and properties of the helical nucleocapsid of the parainfluenza virus SV5. *Proc. Natl. Acad. Sci. USA* **1967**, *57*, 949–956. [CrossRef]
109. Finch, J.T.; Gibbs, A.J. Observations on the Structure of the Nucleocapsids of some Paramyxoviruses. *J. Gen. Virol.* **1970**, *6*, 141–150. [CrossRef]
110. Egelman, E.H.; Wu, S.S.; Amrein, M.; Portner, A.; Murti, G. The Sendai virus nucleocapsid exists in at least four different helical states. *J. Virol.* **1989**, *63*, 2233–2243. [CrossRef]
111. Heggeness, M.H.; Scheid, A.; Choppin, P.W. Conformation of the helical nucleocapsids of paramyxoviruses and vesicular stomatitis virus: Reversible coiling and uncoiling induced by changes in salt concentration. *Proc. Natl. Acad. Sci. USA* **1980**, *77*, 2631–2635. [CrossRef]
112. Bhella, D.; Ralph, A.; Murphy, L.B.; Yeo, R.P. Significant differences in nucleocapsid morphology within the Paramyxoviridae. *J. Gen. Virol.* **2002**, *83*, 1831–1839. [CrossRef]
113. Bhella, D.; Ralph, A.; Yeo, R.P. Conformational Flexibility in Recombinant Measles Virus Nucleocapsids Visualised by Cryo-negative Stain Electron Microscopy and Real-space Helical Reconstruction. *J. Mol. Biol.* **2004**, *340*, 319–331. [CrossRef]
114. Cox, R.; Pickar, A.; Qiu, S.; Tsao, J.; Rodenburg, C.; Dokland, T.; Elson, A.; He, B.; Luo, M. Structural studies on the authentic mumps virus nucleocapsid showing uncoiling by the phosphoprotein. *Proc. Natl. Acad. Sci. USA* **2014**, *111*, 15208–15213. [CrossRef] [PubMed]
115. Ke, Z.; Strauss, J.D.; Hampton, C.M.; Brindley, M.A.; Dillard, R.S.; Leon, F.; Lamb, K.M.; Plemper, R.K.; Wright, E.R. Promotion of virus assembly and organization by the measles virus matrix protein. *Nat. Commun.* **2018**, *9*, 1736. [CrossRef]
116. Nakai, M.; Imagawa, D.T. Electron microscopy of measles virus replication. *J. Virol.* **1969**, *3*, 187–197. [CrossRef]
117. Desfosses, A.; Goret, G.; Estrozi, L.F.; Ruigrok, R.W.H.; Gutsche, I. Nucleoprotein-RNA Orientation in the Measles Virus Nucleocapsid by Three-Dimensional Electron Microscopy. *J. Virol.* **2011**, *85*, 1391–1395. [CrossRef] [PubMed]
118. Spehner, D.; Kirn, A.; Drillien, R. Assembly of nucleocapsidlike structures in animal cells infected with a vaccinia virus recombinant encoding the measles virus nucleoprotein. *J. Virol.* **1991**, *65*, 6296–6300. [CrossRef] [PubMed]
119. Fooks, A.R.; Stephenson, J.R.; Warnes, A.; Dowsett, A.B.; Rima, B.K.; Wilkinson, G.W.G. Measles virus nucleocapsid protein expressed in insect cells assembles into nucleocapsid-like structures. *J. Gen. Virol.* **1993**, *74*, 1439–1444. [CrossRef] [PubMed]
120. Warnes, A.; Fooks, A.R.; Dowsett, A.; Wilkinson, G.W.; Stephenson, J.R. Expression of the measles virus nucleoprotein gene in Escherichia coli and assembly of nucleocapsid-like structures. *Gene* **1995**, *160*, 173–178. [CrossRef]

121. Schoehn, G.; Mavrakis, M.; Albertini, A.; Wade, R.; Hoenger, A.; Ruigrok, R.W. The 12 Å Structure of Trypsin-treated Measles Virus N-RNA. *J. Mol. Biol.* **2004**, *339*, 301–312. [CrossRef] [PubMed]
122. Cox, R.; Green, T.J.; Qiu, S.; Kang, J.; Tsao, J.; Prevelige, P.E.; He, B.; Luo, M. Characterization of a Mumps Virus Nucleocapsidlike Particle. *J. Virol.* **2009**, *83*, 11402–11406. [CrossRef] [PubMed]
123. Rager, M.; Vongpunsawad, S.; Duprex, W.P.; Cattaneo, R. Polyploid measles virus with hexameric genome length. *EMBO J.* **2002**, *21*, 2364–2372. [CrossRef]
124. Loney, C.; Mottet-Osman, G.; Roux, L.; Bhella, D. Paramyxovirus Ultrastructure and Genome Packaging: Cryo-Electron Tomography of Sendai Virus. *J. Virol.* **2009**, *83*, 8191–8197. [CrossRef] [PubMed]
125. Goff, P.H.; Gao, Q.; Palese, P. A Majority of Infectious Newcastle Disease Virus Particles Contain a Single Genome, while a Minority Contain Multiple Genomes. *J. Virol.* **2012**, *86*, 10852–10856. [CrossRef]
126. Shan, H.; Su, X.; Li, T.; Qin, Y.; Zhang, N.; Yang, L.; Ma, L.; Bai, Y.; Qi, L.; Liu, Y.; et al. Structural plasticity of mumps virus nucleocapsids with cryo-EM structures. *Commun. Biol.* **2021**, *4*, 833. [CrossRef]
127. Baronti, L.; Erales, J.; Habchi, J.; Felli, I.C.; Pierattelli, R.; Longhi, S. Dynamics of the Intrinsically Disordered C-Terminal Domain of the Nipah Virus Nucleoprotein and Interaction with the X Domain of the Phosphoprotein as Unveiled by NMR Spectroscopy. *ChemBioChem* **2014**, *16*, 268–276. [CrossRef]
128. Houben, K.; Marion, D.; Tarbouriech, N.; Ruigrok, R.W.H.; Blanchard, L. Interaction of the C-Terminal Domains of Sendai Virus N and P Proteins: Comparison of Polymerase-Nucleocapsid Interactions within the Paramyxovirus Family. *J. Virol.* **2007**, *81*, 6807–6816. [CrossRef] [PubMed]
129. Tawar, R.G.; Duquerroy, S.; Vonrhein, C.; Varela, P.F.; Damier-Piolle, L.; Castagné, N.; MacLellan, K.; Bedouelle, H.; Bricogne, G.; Bhella, D.; et al. Crystal Structure of a Nucleocapsid-Like Nucleoprotein-RNA Complex of Respiratory Syncytial Virus. *Science* **2009**, *326*, 1279–1283. [CrossRef]
130. Bakker, S.E.; Duquerroy, S.; Galloux, M.; Loney, C.; Conner, E.; Eléouët, J.-F.; Rey, F.; Bhella, D. The respiratory syncytial virus nucleoprotein-RNA complex forms a left-handed helical nucleocapsid. *J. Gen. Virol.* **2013**, *94*, 1734–1738. [CrossRef]
131. Renner, M.; Bertinelli, M.; Leyrat, C.; Paesen, G.C.; De Oliveira, L.F.S.; Huiskonen, J.T.; Grimes, J.M. Nucleocapsid assembly in pneumoviruses is regulated by conformational switching of the N protein. *eLife* **2016**, *5*, e12627. [CrossRef]
132. Dong, S.; Yang, P.; Li, G.; Liu, B.; Wang, W.; Liu, X.; Xia, B.; Yang, C.; Lou, Z.; Guo, Y.; et al. Insight into the Ebola virus nucleocapsid assembly mechanism: Crystal structure of Ebola virus nucleoprotein core domain at 1.8 Å resolution. *Protein Cell* **2015**, *6*, 351–362. [CrossRef]
133. Wan, W.; Kolesnikova, L.; Clarke, M.; Koehler, A.; Noda, T.; Becker, S.; Briggs, J.A.G. Structure and assembly of the Ebola virus nucleocapsid. *Nature* **2017**, *551*, 394–397. [CrossRef] [PubMed]
134. Sugita, Y.; Matsunami, H.; Kawaoka, Y.; Noda, T.; Wolf, M. Cryo-EM structure of the Ebola virus nucleoprotein-RNA complex at 3.6 A resolution. *Nature* **2018**, *563*, 137–140. [CrossRef]
135. Su, Z.; Wu, C.; Shi, L.; Luthra, P.; Pintilie, G.D.; Johnson, B.; Porter, J.R.; Ge, P.; Chen, M.; Liu, G.; et al. Electron Cryo-microscopy Structure of Ebola Virus Nucleoprotein Reveals a Mechanism for Nucleocapsid-like Assembly. *Cell* **2018**, *172*, 966–978.e12. [CrossRef]
136. Kirchdoerfer, R.N.; Saphire, E.O.; Ward, A.B. Cryo-EM structure of the Ebola virus nucleoprotein-RNA complex. *Acta Crystallogr. Sect. F Struct. Biol. Commun.* **2019**, *75*, 340–347. [CrossRef]
137. Liu, B.; Dong, S.; Li, G.; Wang, W.; Liu, X.; Wang, Y.; Yang, C.; Rao, Z.; Guo, Y. Structural Insight into Nucleoprotein Conformation Change Chaperoned by VP35 Peptide in Marburg Virus. *J. Virol.* **2017**, *91*, e00825-17. [CrossRef]
138. Rudolph, M.G.; Kraus, I.; Dickmanns, A.; Eickmann, M.; Garten, W.; Ficner, R. Crystal Structure of the Borna Disease Virus Nucleoprotein. *Structure* **2003**, *11*, 1219–1226. [CrossRef] [PubMed]
139. Green, T.J.; Zhang, X.; Wertz, G.W.; Luo, M. Structure of the Vesicular Stomatitis Virus Nucleoprotein-RNA Complex. *Science* **2006**, *313*, 357–360. [CrossRef]
140. Albertini, A.A.V.; Wernimont, A.K.; Muziol, T.M.; Ravelli, R.B.G.; Clapier, C.R.; Schoehn, G.; Weissenhorn, W.; Ruigrok, R.W.H. Crystal Structure of the Rabies Virus Nucleoprotein-RNA Complex. *Science* **2006**, *313*, 360–363. [CrossRef]
141. Luo, M.; Terrell, J.R.; McManus, S.A. Nucleocapsid Structure of Negative Strand RNA Virus. *Viruses* **2020**, *12*, 835. [CrossRef]
142. Ge, P.; Tsao, J.; Schein, S.; Green, T.J.; Luo, M.; Zhou, Z.H. Cryo-EM Model of the Bullet-Shaped Vesicular Stomatitis Virus. *Science* **2010**, *327*, 689–693. [CrossRef]
143. Riedel, C.; Vasishtan, D.; Pražák, V.; Ghanem, A.; Conzelmann, K.-K.; Rümenapf, T. Cryo EM structure of the rabies virus ribonucleoprotein complex. *Sci. Rep.* **2019**, *9*, 9639. [CrossRef]
144. Iseni, F.; Baudin, F.; Garcin, D.; Marq, J.-B.; Ruigrok, R.W.; Kolakofsky, D. Chemical modification of nucleotide bases and mRNA editing depend on hexamer or nucleoprotein phase in Sendai virus nucleocapsids. *RNA* **2002**, *8*, 1056–1067. [CrossRef]
145. Pelet, T.; Delenda, C.; Gubbay, O.; Garcin, D.; Kolakofsky, D. Partial Characterization of a Sendai Virus Replication Promoter and the Rule of Six. *Virology* **1996**, *224*, 405–414. [CrossRef]
146. Tapparel, C.; Maurice, D.; Roux, L. The activity of Sendai virus genomic and antigenomic promoters requires a second element past the leader template regions: A motif (GNNNNN)3 is essential for replication. *J. Virol.* **1998**, *72*, 3117–3128. [CrossRef] [PubMed]
147. Murphy, S.K.; Parks, G.D. RNA replication for the paramyxovirus simian virus 5 requires an internal repeated (CGNNNN) sequence motif. *J. Virol.* **1999**, *73*, 805–809. [CrossRef] [PubMed]

148. Marcos, F.; Ferreira, L.; Cros, J.; Park, M.-S.; Nakaya, T.; García-Sastre, A.; Villar, E. Mapping of the RNA promoter of Newcastle disease virus. *Virology* **2005**, *331*, 396–406. [CrossRef]
149. Matsumoto, Y.; Ohta, K.; Kolakofsky, D.; Nishio, M. A Point Mutation in the RNA-Binding Domain of Human Parainfluenza Virus Type 2 Nucleoprotein Elicits Abnormally Enhanced Polymerase Activity. *J. Virol.* **2017**, *91*, e02203-16. [CrossRef] [PubMed]
150. Matsumoto, Y.; Ohta, K.; Kolakofsky, D.; Nishio, M. The control of paramyxovirus genome hexamer length and mRNA editing. *RNA* **2018**, *24*, 461–467. [CrossRef]
151. Vidal, S.; Curran, J.; Kolakofsky, D. A stuttering model for paramyxovirus P mRNA editing. *EMBO J.* **1990**, *9*, 2017–2022. [CrossRef] [PubMed]
152. Jensen, M.R.; Communie, G.; Ribeiro, E.A.; Martinez, N.; Desfosses, A.; Salmon, L.; Mollica, L.; Gabel, F.; Jamin, M.; Longhi, S.; et al. Intrinsic disorder in measles virus nucleocapsids. *Proc. Natl. Acad. Sci. USA* **2011**, *108*, 9839–9844. [CrossRef]
153. Ryan, K.W.; Portner, A.; Murti, K. Antibodies to Paramyxovirus Nucleoproteins Define Regions Important for Immunogenicity and Nucleocapsid Assembly. *Virology* **1993**, *193*, 376–384. [CrossRef]
154. Zhang, X.; Glendening, C.; Linke, H.; Parks, C.L.; Brooks, C.; Udem, S.A.; Oglesbee, M. Identification and Characterization of a Regulatory Domain on the Carboxyl Terminus of the Measles Virus Nucleocapsid Protein. *J. Virol.* **2002**, *76*, 8737–8746. [CrossRef]
155. Chan, Y.P.; Koh, C.L.; Lam, S.K.; Wang, L.-F. Mapping of domains responsible for nucleocapsid protein-phosphoprotein interaction of henipaviruses. *J. Gen. Virol.* **2004**, *85*, 1675–1684. [CrossRef] [PubMed]
156. Bourhis, J.-M.; Johansson, K.; Receveur-Bréchot, V.; Oldfield, C.J.; Dunker, K.A.; Canard, B.; Longhi, S. The C-terminal domain of measles virus nucleoprotein belongs to the class of intrinsically disordered proteins that fold upon binding to their physiological partner. *Virus Res.* **2004**, *99*, 157–167. [CrossRef] [PubMed]
157. Dosnon, M.; Bonetti, D.; Morrone, A.; Erales, J.; Di Silvio, E.; Longhi, S.; Gianni, S. Demonstration of a Folding after Binding Mechanism in the Recognition between the Measles Virus NTAIL and X Domains. *ACS Chem. Biol.* **2014**, *10*, 795–802. [CrossRef] [PubMed]
158. Coronel, E.C.; Takimoto, T.; Murti, K.G.; Varich, N.; Portner, A. Nucleocapsid Incorporation into Parainfluenza Virus Is Regulated by Specific Interaction with Matrix Protein. *J. Virol.* **2001**, *75*, 1117–1123. [CrossRef]
159. Iwasaki, M.; Takeda, M.; Shirogane, Y.; Nakatsu, Y.; Nakamura, T.; Yanagi, Y. The matrix protein of measles virus regulates viral RNA synthesis and assembly by interacting with the nucleocapsid protein. *J. Virol.* **2009**, *83*, 10374–10383. [CrossRef]
160. Schmitt, P.T.; Ray, G.; Schmitt, A. The C-Terminal End of Parainfluenza Virus 5 NP Protein Is Important for Virus-Like Particle Production and M-NP Protein Interaction. *J. Virol.* **2010**, *84*, 12810–12823. [CrossRef]
161. Liljeroos, L.; Huiskonen, J.; Ora, A.; Susi, P.; Butcher, S.J. Electron cryotomography of measles virus reveals how matrix protein coats the ribonucleocapsid within intact virions. *Proc. Natl. Acad. Sci. USA* **2011**, *108*, 18085–18090. [CrossRef]
162. Ray, G.; Schmitt, P.T.; Schmitt, A.P. C-Terminal DxD-Containing Sequences within Paramyxovirus Nucleocapsid Proteins Determine Matrix Protein Compatibility and Can Direct Foreign Proteins into Budding Particles. *J. Virol.* **2016**, *90*, 3650–3660. [CrossRef]
163. Zhang, X.; Bourhis, J.-M.; Longhi, S.; Carsillo, T.; Buccellato, M.; Morin, B.; Canard, B.; Oglesbee, M. Hsp72 recognizes a P binding motif in the measles virus N protein C-terminus. *Virology* **2005**, *337*, 162–174. [CrossRef]
164. Couturier, M.; Buccellato, M.; Costanzo, S.; Bourhis, J.-M.; Shu, Y.; Nicaise, M.; Desmadril, M.; Flaudrops, C.; Longhi, S.; Oglesbee, M. High affinity binding between Hsp70 and the C-terminal domain of the measles virus nucleoprotein requires an Hsp40 co-chaperone. *J. Mol. Recognit.* **2009**, *23*, 301–315. [CrossRef]
165. Watanabe, A.; Yoneda, M.; Ikeda, F.; Sugai, A.; Sato, H.; Kai, C. Peroxiredoxin 1 Is Required for Efficient Transcription and Replication of Measles Virus. *J. Virol.* **2010**, *85*, 2247–2253. [CrossRef]
166. Mavrakis, M.; Méhouas, S.; Réal, E.; Iseni, F.; Blondel, D.; Tordo, N.; Ruigrok, R.W. Rabies virus chaperone: Identification of the phosphoprotein peptide that keeps nucleoprotein soluble and free from non-specific RNA. *Virology* **2006**, *349*, 422–429. [CrossRef]
167. Karlin, D.; Belshaw, R. Detecting Remote Sequence Homology in Disordered Proteins: Discovery of Conserved Motifs in the N-Termini of *Mononegavirales* phosphoproteins. *PLoS ONE* **2012**, *7*, e31719. [CrossRef]
168. Leyrat, C.; Yabukarski, F.; Tarbouriech, N.; Ribeiro, E.A., Jr.; Jensen, M.R.; Blackledge, M.; Ruigrok, R.W.H.; Jamin, M. Structure of the Vesicular Stomatitis Virus N0-P Complex. *PLoS Pathog.* **2011**, *7*, e1002248. [CrossRef]
169. Kirchdoerfer, R.N.; Abelson, D.M.; Li, S.; Wood, M.R.; Saphire, E.O. Assembly of the Ebola Virus Nucleoprotein from a Chaperoned VP35 Complex. *Cell Rep.* **2015**, *12*, 140–149. [CrossRef]
170. Leung, D.W.; Borek, D.; Luthra, P.; Binning, J.M.; Anantpadma, M.; Liu, G.; Harvey, I.B.; Su, Z.; Endlich-Frazier, A.; Pan, J.; et al. An Intrinsically Disordered Peptide from Ebola Virus VP35 Controls Viral RNA Synthesis by Modulating Nucleoprotein-RNA Interactions. *Cell Rep.* **2015**, *11*, 376–389. [CrossRef]
171. Zhu, T.; Song, H.; Peng, R.; Shi, Y.; Qi, J.; Gao, G.F. Crystal Structure of the Marburg Virus Nucleoprotein Core Domain Chaperoned by a VP35 Peptide Reveals a Conserved Drug Target for Filovirus. *J. Virol.* **2017**, *91*, e00996-17. [CrossRef]
172. Landeras-Bueno, S.; Oda, S.-I.; Norris, M.J.; Salie, Z.L.; Guenaga, J.; Wyatt, R.T.; Saphire, E.O. Sudan Ebolavirus VP35-NP Crystal Structure Reveals a Potential Target for Pan-Filovirus Treatment. *mBio* **2019**, *10*, e00734-19. [CrossRef]
173. Milles, S.; Jensen, M.R.; Lazert, C.; Guseva, S.; Ivashchenko, S.; Communie, G.; Maurin, D.; Gerlier, D.; Ruigrok, R.W.H.; Blackledge, M. An ultraweak interaction in the intrinsically disordered replication machinery is essential for measles virus function. *Sci. Adv.* **2018**, *4*, eaat7778. [CrossRef]

174. Schiavina, M.; Salladini, E.; Murrali, M.G.; Tria, G.; Felli, I.C.; Pierattelli, R.; Longhi, S. Ensemble description of the intrinsically disordered N-terminal domain of the Nipah virus P/V protein from combined NMR and SAXS. *Sci. Rep.* **2020**, *10*, 19574. [CrossRef]
175. Cevik, B.; Kaesberg, J.; Smallwood, S.; Feller, J.A.; Moyer, S.A. Mapping the phosphoprotein binding site on Sendai virus NP protein assembled into nucleocapsids. *Virology* **2004**, *325*, 216–224. [CrossRef]
176. Milles, S.; Jensen, M.R.; Communie, G.; Maurin, D.; Schoehn, G.; Ruigrok, R.W.; Blackledge, M. Self-Assembly of Measles Virus Nucleocapsid-like Particles: Kinetics and RNA Sequence Dependence. *Angew. Chem. Int. Ed.* **2016**, *55*, 9356–9360. [CrossRef]
177. Blumberg, B.M.; Giorgi, C.; Kolakofsky, D. N protein of vesicular stomatitis virus selectively encapsidates leader RNA in vitro. *Cell* **1983**, *32*, 559–567. [CrossRef]
178. Moyer, S.A.; Smallwood-Kentro, S.; Haddad, A.; Prevec, L. Assembly and transcription of synthetic vesicular stomatitis virus nucleocapsids. *J. Virol.* **1991**, *65*, 2170–2178. [CrossRef]
179. Green, T.J.; Rowse, M.; Tsao, J.; Kang, J.; Ge, P.; Zhou, Z.H.; Luo, M. Access to RNA Encapsidated in the Nucleocapsid of Vesicular Stomatitis Virus. *J. Virol.* **2010**, *85*, 2714–2722. [CrossRef]
180. Gao, Y.; Cao, D.; Ahn, H.M.; Swain, A.; Hill, S.; Ogilvie, C.; Kurien, M.; Rahmatullah, T.; Liang, B. In vitro trackable assembly of RNA-specific nucleocapsids of the respiratory syncytial virus. *J. Biol. Chem.* **2020**, *295*, 883–895. [CrossRef]
181. Guseva, S.; Milles, S.; Jensen, M.R.; Salvi, N.; Kleman, J.-P.; Maurin, D.; Ruigrok, R.W.H.; Blackledge, M. Measles virus nucleo- and phosphoproteins form liquid-like phase-separated compartments that promote nucleocapsid assembly. *Sci. Adv.* **2020**, *6*, eaaz7095. [CrossRef]
182. Gérard, F.C.A.; Jamin, M.; Blackledge, M.; Blondel, D.; Bourhis, J.-M. Vesicular Stomatitis Virus Phosphoprotein Dimerization Domain Is Dispensable for Virus Growth. *J. Virol.* **2020**, *94*, e01789-19. [CrossRef] [PubMed]
183. Bloyet, L.-M.; Morin, B.; Brusic, V.; Gardner, E.; Ross, R.A.; Vadakkan, T.; Kirchhausen, T.; Whelan, S.P.J. Oligomerization of the Vesicular Stomatitis Virus Phosphoprotein Is Dispensable for mRNA Synthesis but Facilitates RNA Replication. *J. Virol.* **2020**, *94*, e00115-20. [CrossRef] [PubMed]
184. Curran, J. A role for the Sendai virus P protein trimer in RNA synthesis. *J. Virol.* **1998**, *72*, 4274–4280. [CrossRef]
185. Kolakofsky, D.; Le Mercier, P.; Iseni, F.; Garcin, D. Viral DNA polymerase scanning and the gymnastics of Sendai virus RNA synthesis. *Virology* **2004**, *318*, 463–473. [CrossRef]
186. Kingston, R.L.; Gay, L.S.; Baase, W.S.; Matthews, B.W. Structure of the Nucleocapsid-Binding Domain from the Mumps Virus Polymerase; an Example of Protein Folding Induced by Crystallization. *J. Mol. Biol.* **2008**, *379*, 719–731. [CrossRef]
187. Gely, S.; Lowry, D.F.; Bernard, C.; Jensen, M.R.; Blackledge, M.; Costanzo, S.; Bourhis, J.-M.; Darbon, H.; Daughdrill, G.; Longhi, S. Solution structure of the C-terminal X domain of the measles virus phosphoprotein and interaction with the intrinsically disordered C-terminal domain of the nucleoprotein. *J. Mol. Recognit.* **2010**, *23*, 435–447. [CrossRef]
188. Bloyet, L.-M.; Schramm, A.; Lazert, C.; Raynal, B.; Hologne, M.; Walker, O.; Longhi, S.; Gerlier, D. Regulation of measles virus gene expression by P protein coiled-coil properties. *Sci. Adv.* **2019**, *5*, eaaw3702. [CrossRef] [PubMed]
189. Du Pont, V.; Jiang, Y.; Plemper, R.K. Bipartite interface of the measles virus phosphoprotein X domain with the large polymerase protein regulates viral polymerase dynamics. *PLoS Pathog.* **2019**, *15*, e1007995. [CrossRef] [PubMed]
190. Kingston, R.L.; Baase, W.A.; Gay, L.S. Characterization of nucleocapsid binding by the measles virus and mumps virus phosphoproteins. *J. Virol.* **2004**, *78*, 8630–8640. [CrossRef]
191. Sourimant, J.; Thakkar, V.D.; Cox, R.M.; Plemper, R.K. Viral evolution identifies a regulatory interface between paramyxovirus polymerase complex and nucleocapsid that controls replication dynamics. *Sci. Adv.* **2020**, *6*, eaaz1590. [CrossRef] [PubMed]
192. Omi-Furutani, M.; Yoneda, M.; Fujita, K.; Ikeda, F.; Kai, C. Novel Phosphoprotein-Interacting Region in Nipah Virus Nucleocapsid Protein and Its Involvement in Viral Replication. *J. Virol.* **2010**, *84*, 9793–9799. [CrossRef] [PubMed]
193. Yegambaram, K.; Kingston, R.L. The feet of the measles virus polymerase bind the viral nucleocapsid protein at a single site. *Protein Sci.* **2010**, *19*, 893–899. [CrossRef]
194. Bourhis, J.-M.; Receveur-Brechot, V.; Oglesbee, M.; Zhang, X.; Buccellato, M.; Darbon, H.; Canard, B.; Finet, S.; Longhi, S. The intrinsically disordered C-terminal domain of the measles virus nucleoprotein interacts with the C-terminal domain of the phosphoprotein via two distinct sites and remains predominantly unfolded. *Protein Sci.* **2005**, *14*, 1975–1992. [CrossRef]
195. Belle, V.; Rouger, S.; Costanzo, S.; Liquière, E.; Strancar, J.; Guigliarelli, B.; Fournel, A.; Longhi, S. Mapping α-helical induced folding within the intrinsically disordered C-terminal domain of the measles virus nucleoprotein by site-directed spin-labeling EPR spectroscopy. *Proteins Struct. Funct. Bioinform.* **2008**, *73*, 973–988. [CrossRef]
196. Kavalenka, A.; Urbancic, I.; Belle, V.; Rouger, S.; Costanzo, S.; Kure, S.; Fournel, A.; Longhi, S.; Guigliarelli, B.; Strancar, J. Conformational analysis of the partially disordered measles virus N(TAIL)-XD complex by SDSL EPR spectroscopy. *Biophys. J.* **2010**, *98*, 1055–1064. [CrossRef]
197. Martinho, M.; Habchi, J.; El Habre, Z.; Nesme, L.; Guigliarelli, B.; Belle, V.; Longhi, S. Assessing induced folding within the intrinsically disordered C-terminal domain of the Henipavirus nucleoproteins by site-directed spin labeling EPR spectroscopy. *J. Biomol. Struct. Dyn.* **2013**, *31*, 453–471. [CrossRef]
198. Tompa, P.; Fuxreiter, M. Fuzzy complexes: Polymorphism and structural disorder in protein-protein interactions. *Trends Biochem. Sci.* **2008**, *33*, 2–8. [CrossRef]
199. Gruet, A.; Dosnon, M.; Blocquel, D.; Brunel, J.; Gerlier, D.; Das, R.; Bonetti, D.; Gianni, S.; Fuxreiter, M.; Longhi, S.; et al. Fuzzy regions in an intrinsically disordered protein impair protein-protein interactions. *FEBS J.* **2016**, *283*, 576–594. [CrossRef]

200. Troilo, F.; Bonetti, D.; Bignon, C.; Longhi, S.; Gianni, S. Understanding Intramolecular Crosstalk in an Intrinsically Disordered Protein. *ACS Chem. Biol.* **2019**, *14*, 337–341. [CrossRef] [PubMed]
201. Gruet, A.; Dosnon, M.; Vassena, A.; Lombard, V.; Gerlier, D.; Bignon, C.; Longhi, S. Dissecting Partner Recognition by an Intrinsically Disordered Protein Using Descriptive Random Mutagenesis. *J. Mol. Biol.* **2013**, *425*, 3495–3509. [CrossRef]
202. Shu, Y.; Habchi, J.; Costanzo, S.; Padilla, A.; Brunel, J.; Gerlier, D.; Oglesbee, M.; Longhi, S. Plasticity in Structural and Functional Interactions between the Phosphoprotein and Nucleoprotein of Measles Virus. *J. Biol. Chem.* **2012**, *287*, 11951–11967. [CrossRef]
203. Brunel, J.; Chopy, D.; Dosnon, M.; Bloyet, L.-M.; Devaux, P.; Urzua, E.; Cattaneo, R.; Longhi, S.; Gerlier, D. Sequence of Events in Measles Virus Replication: Role of Phosphoprotein-Nucleocapsid Interactions. *J. Virol.* **2014**, *88*, 10851–10863. [CrossRef] [PubMed]
204. Bloyet, L.-M.; Brunel, J.; Dosnon, M.; Hamon, V.; Erales, J.; Gruet, A.; Lazert, C.; Bignon, C.; Roche, P.; Longhi, S.; et al. Modulation of Re-initiation of Measles Virus Transcription at Intergenic Regions by PXD to NTAIL Binding Strength. *PLoS Pathog.* **2016**, *12*, e1006058. [CrossRef] [PubMed]
205. Krumm, S.A.; Takeda, M.; Plemper, R.K. The Measles Virus Nucleocapsid Protein Tail Domain Is Dispensable for Viral Polymerase Recruitment and Activity. *J. Biol. Chem.* **2013**, *288*, 29943–29953. [CrossRef] [PubMed]
206. Thakkar, V.; Cox, R.M.; Sawatsky, B.; Budaszewski, R.D.F.; Sourimant, J.; Wabbel, K.; Makhsous, N.; Greninger, A.; von Messling, V.; Plemper, R.K. The Unstructured Paramyxovirus Nucleocapsid Protein Tail Domain Modulates Viral Pathogenesis through Regulation of Transcriptase Activity. *J. Virol.* **2018**, *92*, e02064-17. [CrossRef] [PubMed]
207. Cox, R.M.; Krumm, S.A.; Thakkar, V.D.; Sohn, M.; Plemper, R.K. The structurally disordered paramyxovirus nucleocapsid protein tail domain is a regulator of the mRNA transcription gradient. *Sci. Adv.* **2017**, *3*, e1602350. [CrossRef] [PubMed]
208. Galloux, M.; Tarus, B.; Blazevic, I.; Fix, J.; Duquerroy, S.; Eléouët, J.-F. Characterization of a Viral Phosphoprotein Binding Site on the Surface of the Respiratory Syncytial Nucleoprotein. *J. Virol.* **2012**, *86*, 8375–8387. [CrossRef]
209. Ouizougun-Oubari, M.; Pereira, N.; Tarus, B.; Galloux, M.; Lassoued, S.; Fix, J.; Tortorici, M.A.; Hoos, S.; Baron, B.; England, P.; et al. A Druggable Pocket at the Nucleocapsid/Phosphoprotein Interaction Site of Human Respiratory Syncytial Virus. *J. Virol.* **2015**, *89*, 11129–11143. [CrossRef] [PubMed]
210. Green, T.J.; Luo, M. Structure of the vesicular stomatitis virus nucleocapsid in complex with the nucleocapsid-binding domain of the small polymerase cofactor, P. *Proc. Natl. Acad. Sci. USA* **2009**, *106*, 11713–11718. [CrossRef]
211. Oglesbee, M.J.; Liu, Z.; Kenney, H.; Brooks, C.L. The Highly Inducible Member of the 70 kDa Family of Heat Shock Proteins Increases Canine Distemper Virus Polymerase Activity. *J. Gen. Virol.* **1996**, *77*, 2125–2135. [CrossRef]
212. Oglesbee, M.; Tatalick, L.; Rice, J.; Krakowka, S. Isolation and Characterization of Canine Distemper Virus Nucleocapsid Variants. *J. Gen. Virol.* **1989**, *70*, 2409–2419. [CrossRef]
213. Oglesbee, M.; Ringler, S.; Krakowka, S. Interaction of canine distemper virus nucleocapsid variants with 70K heat-shock proteins. *J. Gen. Virol.* **1990**, *71*, 1585–1590. [CrossRef] [PubMed]
214. Jamin, M.; Yabukarski, F. Nonsegmented Negative-Sense RNA Viruses—Structural Data Bring New Insights into Nucleocapsid Assembly. *Adv. Virus Res.* **2017**, *97*, 143–185. [CrossRef]
215. Severin, C.; Terrell, J.R.; Zengel, J.R.; Cox, R.; Plemper, R.K.; He, B.; Luo, M. Releasing the Genomic RNA Sequestered in the Mumps Virus Nucleocapsid. *J. Virol.* **2016**, *90*, 10113–10119. [CrossRef] [PubMed]
216. Curran, J. Reexamination of the Sendai Virus P Protein Domains Required for RNA Synthesis: A Possible Supplemental Role for the P Protein. *Virology* **1996**, *221*, 130–140. [CrossRef]
217. De, B.P.; Hoffman, M.A.; Choudhary, S.; Huntley, C.C.; Banerjee, A.K. Role of NH_2- and COOH-Terminal Domains of the P Protein of Human Parainfluenza Virus Type 3 in Transcription and Replication. *J. Virol.* **2000**, *74*, 5886–5895. [CrossRef]
218. Ogino, T.; Green, T.J. RNA Synthesis and Capping by Non-segmented Negative Strand RNA Viral Polymerases: Lessons from a Prototypic Virus. *Front. Microbiol.* **2019**, *10*, 1490. [CrossRef] [PubMed]